Physics – Uspekhi **59** (7) 619 – 641 (2016)

REVIEWS OF TOPICAL PROBLEMS PACS numbers: 12.20.Ds, **32.80.–t**

Quantum electrodynamics processes in the interaction of high-energy particles with atoms

P A Krachkov, R N Lee, A I Milstein

DOI: 10.3367/UFNe.2016.03.037743

Contents

Abstract. **The recently developed method of quasiclassical Green's functions of the Dirac equation in the variously configured external fields has provided breakthrough insight into fundamental quantum electrodynamics processes whereby high-energy particles interact with atoms. This paper reviews latest calculated results, exact in the atomic field parameters, on the cross sections for electron–positron high-energy photoproduction, the single bremsstrahlung cross section for relativistic electrons and muons in an atomic field, double bremsstrahlung cross sections, etc. In many cases, the calculations are performed in the quasiclassical approximation with the inclusion of the first-order quasiclassical correction.**

Keywords: quantum electrodynamics, strong field, photoproduction, bremsstrahlung

P A Krachkov, R N Lee, A I Milstein Budker Institute of Nuclear Physics, Siberian Branch of the Russian Academy of Sciences, prosp. Akademika Lavrent'eva 11, 630090 Novosibirsk, Russian Federation
E-mail: peter_phys@mail.ru, r.n.lee@inp.nsk.su, a.i.milstein@inp.nsk.su

Received 21 January 2016
Uspekhi Fizicheskikh Nauk **186** (7) 689 – 711 (2016)
DOI: 10.3367/UFNr.2016.03.037743
Translated by Yu V Morozov; edited by A Radzig

In memory to Vladimir Nikolaevich Baier

1. Introduction

Only a few years separate the publication of the famous Dirac equation [1] and the first reports [2, 3] on the investigation, in the framework of this equation, of fundamental quantum electrodynamics processes in an atomic field. In these studies, consideration was in a leading order of perturbation theory in the fine-structure constant α and the parameter $\eta = Z\alpha$ (Z is the atomic number). The accuracy of results obtained in the lowest order in η (referred to below as Born results) is not very high even at relatively small Z values; therefore, it is often necessary for applications that the dependence on η be taken into account exactly. The difference between a result exact in η and a Born result is called the Coulomb correction. Unfortunately, the solution of the Dirac equation for a relativistic particle in the Coulomb field, necessary to calculate cross sections of various processes, can be written out only as the sum over angular momenta [4], unlike the solution of the Schrödinger equation in the Coulomb field, for which a simple closed-form expression exists.

For ultrarelativistic particles, the main contribution to cross sections usually comes from small angles θ between the momenta of initial and final particles. In such a case, the characteristic angular momentum l_c can be estimated as $l_c \sim p\rho$, where p is the characteristic momentum, $\rho \sim 1/\delta p$ is the characteristic impact parameter, and $\delta p \sim p\theta$ is the characteristic momentum transfer ($\hbar = c = 1$). In other words, $l_c \sim 1/\theta \gg 1$. This makes the use of these expressions for numerical calculations, even at relatively small energies, extremely difficult [6], even though there are formal expressions for cross sections of pair photoproduction and bremsstrahlung in the Coulomb field that hold for any energies and values of parameter $\eta < 1$ [5]. The difficulties become insurmountable at high particle energies. Fortunately, the quasiclassical approximation can be applied at small scattering angles, which allows taking into account the contribution of large angular momenta to process amplitudes.

An important step in the application of the quasiclassical approximation to research on photoproduction and bremsstrahlung in an atomic field exactly in η was made in Refs [7–9], where a simple expression for Coulomb corrections to the cross sections of these processes was derived. However, such expressions are sufficiently accurate only at very high energies ($\varepsilon \gtrsim 100$ MeV). The authors of Refs [7–9] used wave functions in the Furry–Sommerfeld–Maue approximation [10, 11]. It will be shown below that these are wave functions of electrons in the Coulomb field, calculated in the leading quasiclassical approximation.

The next step in the development of the quasiclassical approach to the investigation of quantum electrodynamics processes in the external fields was the operator quasiclassical technique proposed by V N Baier and V M Katkov [12]. It allowed not only markedly simplifying the derivation of the previous results but also obtaining many important new results [13] in the leading quasiclassical approximation. However, this approach does not allow calculating the quasiclassical corrections to the results obtained in the leading quasiclassical approximation (corrections in $1/l_c \sim \theta \ll 1$). This difficulty was overcome in the method of quasiclassical Green's functions of the Dirac equation in an electromagnetic field. The importance of this method is connected with the possibility of calculating not only the leading contribution to cross sections but also the first-order quasiclassical correction to it. Moreover, analytical results can be obtained in the framework of this method even in the absence of the exact analytical solution to the Dirac equation for a given electromagnetic field. Quasiclassical Green's functions were obtained for the Coulomb field in Refs [14, 15], for an arbitrary spherically symmetrical field in Refs [16, 17], for an arbitrarily localized field [18], and for the superposition of a strong laser field and the atomic field in Ref. [19]. References [18, 20] report on the first-order calculated corrections to all matrix structures of quasiclassical Green's function for an arbitrary spherically symmetrical localized field. Quasiclassical Green's functions were employed to derive simple formulas for the differential cross section of Delbrück scattering at high energies (elastic photon scattering on an atom due to production of a virtual electron–positron pair) and to correctly calculate for the first time the total cross section of this process [21] most accurately measured in Ref. [22]. Moreover, the implementation of quasiclassical Green's functions made it possible to calculate (also for the first time) the cross section of high-energy photon splitting in the atomic field [23]. This effect was first examined experimentally in paper [24]. Consideration of corrections to quasiclassical Green's functions and the corresponding wave functions enhanced considerably the accuracy of calculations of cross sections of such fundamental quantum electrodynamics processes as pair photoproduction and bremsstrahlung in an atomic field and allowed for the first time quantitatively predicting charge asymmetry in these processes at high energies (the change in cross sections upon positron substitution for an electron). The processes of photoproduction and bremsstrahlung are of primary importance for the description of electromagnetic showers in detectors and constitute a noticeable background in the search for new physics in precision experiments. Therefore, cross sections of these processes need to be determined to a high degree of accuracy. The present review was designed to consider current trends in the theory of photoproduction and bremsstrahlung in high-energy processes.

2. Quasiclassical Green's functions and wave functions of the Dirac equation

Similar to the case of an equation of free motion, the particle propagator in the external field coincides with the Green's function of the corresponding wave equation. Because the momentum is not conserved in the coordinate-dependent external field, the distinguished role of momentum representation disappears and all calculations are, as a rule, made in the coordinate representation. The Green's function of the Dirac equation in potential $V(r)$ can be given as

$$G(\mathbf{r}_2, \mathbf{r}_1|\varepsilon) = (\hat{\mathcal{P}} + m)\, D(\mathbf{r}_2, \mathbf{r}_1|\varepsilon)\,,$$
$$D(\mathbf{r}_2, \mathbf{r}_1|\varepsilon) = \left\langle \mathbf{r}_2 \left| \frac{1}{\hat{\mathcal{P}}^2 - m^2 + \mathrm{i}0} \right| \mathbf{r}_1 \right\rangle , \tag{1}$$

where m is the electron mass, $\hat{\mathcal{P}} = \gamma^\nu \mathcal{P}_\nu$, with $\mathcal{P}_\nu = (\varepsilon - V(r), \mathrm{i}\boldsymbol{\nabla})$, γ^ν is the Dirac matrix, and $D(\mathbf{r}_2, \mathbf{r}_1|\varepsilon)$ is the Green's function of the Dirac equation squared. Since the function $D(\mathbf{r}_2, \mathbf{r}_1|\varepsilon)$ contains an even number of gamma matrices, it can be written out in the form

$$D(\mathbf{r}_2, \mathbf{r}_1|\varepsilon) = d_0(\mathbf{r}_2, \mathbf{r}_1|\varepsilon) + \boldsymbol{\alpha}\mathbf{d}_1(\mathbf{r}_2, \mathbf{r}_1|\varepsilon) + \boldsymbol{\Sigma}\mathbf{d}_2(\mathbf{r}_2, \mathbf{r}_1|\varepsilon) + \gamma^5 d_3(\mathbf{r}_2, \mathbf{r}_1|\varepsilon)\,, \tag{2}$$

where $\boldsymbol{\alpha} = \gamma^0\boldsymbol{\gamma}$, $\boldsymbol{\Sigma} = \gamma^0\gamma^5\boldsymbol{\gamma}$, and $d_i(\mathbf{r}_2, \mathbf{r}_1|\varepsilon)$ are certain functions. For the spherically symmetric potential, coefficient $d_3(\mathbf{r}_2, \mathbf{r}_1|\varepsilon)$ equals zero, because it must be a pseudoscalar by virtue of parity conservation, but a pseudoscalar cannot be constructed from two vectors, $\mathbf{r}_1$ and $\mathbf{r}_2$. Once function $D(\mathbf{r}_2, \mathbf{r}_1|\varepsilon)$ is known, it is easy to find positive frequency and negative frequency solutions, $u_{\mathbf{p}}^{\pm}(\mathbf{r})$ and $v_{\mathbf{p}}^{\pm}(\mathbf{r})$, of the Dirac equation using relations [25]:

$$\frac{\exp(\mathrm{i}pr_1)}{4\pi r_1}\, u_{\mathbf{p}}^{+}(\mathbf{r}_2) = -\lim_{r_1\to\infty} D(\mathbf{r}_2, \mathbf{r}_1|\varepsilon_p) u_{\mathbf{p}}\,, \quad \mathbf{p} = -p\mathbf{n}_1\,,$$
$$\frac{\exp(\mathrm{i}pr_2)}{4\pi r_2}\, \bar{u}_{\mathbf{p}}^{-}(\mathbf{r}_1) = -\lim_{r_2\to\infty} \bar{u}_{\mathbf{p}} D(\mathbf{r}_2, \mathbf{r}_1|\varepsilon_p)\,, \quad \mathbf{p} = p\mathbf{n}_2\,,$$
$$\frac{\exp(\mathrm{i}pr_1)}{4\pi r_1}\, v_{\mathbf{p}}^{+}(\mathbf{r}_2) = -\lim_{r_1\to\infty} D(\mathbf{r}_2, \mathbf{r}_1|-\varepsilon_p) v_{\mathbf{p}}\,, \quad \mathbf{p} = p\mathbf{n}_1\,,$$
$$\frac{\exp(\mathrm{i}pr_2)}{4\pi r_2}\, \bar{v}_{\mathbf{p}}^{-}(\mathbf{r}_1) = -\lim_{r_2\to\infty} \bar{v}_{\mathbf{p}} D(\mathbf{r}_2, \mathbf{r}_1|-\varepsilon_p)\,, \quad \mathbf{p} = -p\mathbf{n}_2\,, \tag{3}$$

where $\mathbf{n}_1 = \mathbf{r}_1/r_1$, $\mathbf{n}_2 = \mathbf{r}_2/r_2$, $\varepsilon_p = \sqrt{p^2 + m^2}$, and $u_{\mathbf{p}}$ and $v_{\mathbf{p}}$ are the positive frequency and negative frequency Dirac spinors. The asymptotics of solutions $u_{\mathbf{p}}^{+}(\mathbf{r})$ and $v_{\mathbf{p}}^{+}(\mathbf{r})$ at large distances contain a plain wave and a diverging spherical wave, while the asymptotics of solutions $u_{\mathbf{p}}^{-}(\mathbf{r})$ and $v_{\mathbf{p}}^{-}(\mathbf{r})$ at large distances contain a plain wave and a converging spherical wave. It follows from formulas (2) and (3) that wave functions take the form

$$\begin{aligned}
\bar{u}_{\mathbf{p}}^{-}(\mathbf{r}) &= \bar{u}_{\mathbf{p}}\big[f_0(\mathbf{r},\mathbf{p}) - \boldsymbol{\alpha}\,\mathbf{f}_1(\mathbf{r},\mathbf{p}) - \boldsymbol{\Sigma}\,\mathbf{f}_2(\mathbf{r},\mathbf{p})\big]\,,\\
u_{\mathbf{p}}^{+}(\mathbf{r}) &= \big[f_0(\mathbf{r},-\mathbf{p}) - \boldsymbol{\alpha}\,\mathbf{f}_1(\mathbf{r},-\mathbf{p}) + \boldsymbol{\Sigma}\,\mathbf{f}_2(\mathbf{r},-\mathbf{p})\big]u_{\mathbf{p}}\,,\\
v_{\mathbf{p}}^{+}(\mathbf{r}) &= \big[g_0(\mathbf{r},\mathbf{p}) + \boldsymbol{\alpha}\,\mathbf{g}_1(\mathbf{r},\mathbf{p}) + \boldsymbol{\Sigma}\,\mathbf{g}_2(\mathbf{r},\mathbf{p})\big]v_{\mathbf{p}}\,,\\
\bar{v}_{\mathbf{p}}^{-}(\mathbf{r}) &= \bar{v}_{\mathbf{p}}\big[g_0(\mathbf{r},-\mathbf{p}) + \boldsymbol{\alpha}\,\mathbf{g}_1(\mathbf{r},-\mathbf{p}) - \boldsymbol{\Sigma}\,\mathbf{g}_2(\mathbf{r},-\mathbf{p})\big]\,.
\end{aligned} \tag{4}$$

Coefficients g_i differ from f_i by the substitution $V(r) \to -V(r)$.

Coefficients d_0, $\mathbf{d}_1$, f_0, and $\mathbf{f}_1$ for the arbitrarily localized potential $V(r)$ were calculated in Ref. [18] in the leading quasiclassical approximation, together with the first-order quasiclassical corrections to coefficients d_0 and f_0. The first-order quasiclassical corrections to coefficients $\mathbf{d}_1$ and $\mathbf{f}_1$ were calculated in Ref. [20], together with the leading quasiclassical contribution to $\mathbf{d}_2$ and $\mathbf{f}_2$. Notice that the relative value of coefficients f_0, $\mathbf{f}_{1,2}$, d_0, and $\mathbf{d}_{1,2}$ is different:

$$f_0 \sim l_{\mathrm{c}} f_1 \sim l_{\mathrm{c}}^2 f_2\,, \qquad d_0 \sim l_{\mathrm{c}}\, d_1 \sim l_{\mathrm{c}}^2 d_2\,. \tag{5}$$

Here, $l_{\mathrm{c}} \sim 1/\theta \gg 1$ is the characteristic angular momentum in the process. Since the coefficients are multiplied by different matrices, due to cancellations in bremsstrahlung and photoproduction matrix elements, in order to calculate the first-order quasiclassical correction to the cross section, it is necessary to take account of the first-order quasiclassical correction to coefficients f_0, $\mathbf{f}_1$, d_0, and $\mathbf{d}_1$, while coefficients $\mathbf{f}_2$ and $\mathbf{d}_2$ can be taken into consideration in the leading quasiclassical approximation.

Given that the first-order quasiclassical correction is taken into account, coefficients d_0 and $\mathbf{d}_1$ have the form [18, 20]

$$\begin{aligned}
d_0(\mathbf{r}_2,\mathbf{r}_1|\varepsilon) &= \frac{\mathrm{i}\exp(\mathrm{i}\kappa r)}{4\pi^2 r}\\
&\times\int \mathrm{d}\mathbf{Q}\left(1+\frac{\mathrm{i}r^3}{2\kappa}\int_0^1 \mathrm{d}x\int_0^x \mathrm{d}y\,(x-y)\boldsymbol{\nabla}_\perp V(\mathbf{R}_x)\boldsymbol{\nabla}_\perp V(\mathbf{R}_y)\right)\mathcal{T},\\
\mathbf{d}_1(\mathbf{r}_2,\mathbf{r}_1|\varepsilon) &= -\frac{\mathrm{i}}{2\varepsilon}(\boldsymbol{\nabla}_1+\boldsymbol{\nabla}_2)d_0(\mathbf{r}_2,\mathbf{r}_1|\,\varepsilon)\\
&\quad-\frac{\mathrm{i}\exp(\mathrm{i}\kappa r)}{16\pi^2\varepsilon^2}\int \mathrm{d}\mathbf{Q}\int_0^1 \mathrm{d}x\,\boldsymbol{\nabla}V^2(\mathbf{R}_x)\,\mathcal{T}\,,\\
\mathcal{T} &= \exp\left(\mathrm{i}Q^2 - \mathrm{i}r\int_0^1 \mathrm{d}x\,V(\mathbf{R}_x)\right), \quad \mathbf{r} = \mathbf{r}_2 - \mathbf{r}_1\,,\\
\mathbf{R}_x &= \mathbf{r}_1 + x\mathbf{r} + \mathbf{Q}\sqrt{\frac{2r_1r_2}{\kappa r}}\,,
\end{aligned} \tag{6}$$

where $\kappa = \sqrt{\varepsilon^2 - m^2}$, $\mathbf{Q}$ is the two-dimensional vector normal to vector $\mathbf{r}$, and $\boldsymbol{\nabla}_\perp$ is the gradient component perpendicular to $\mathbf{r}$. Coefficient $\mathbf{d}_2$ was also obtained in Ref. [20] in the leading approximation:

$$\begin{aligned}
\mathbf{d}_2(\mathbf{r}_2,\mathbf{r}_1|\varepsilon) &= -\frac{r\exp(\mathrm{i}\kappa r)}{16\pi^2\varepsilon^2}\\
&\times\int \mathrm{d}\mathbf{Q}\int_0^1 \mathrm{d}x\int_0^x \mathrm{d}y\,\big[\boldsymbol{\nabla}V(\mathbf{R}_x)\times\boldsymbol{\nabla}V(\mathbf{R}_y)\big]\,\mathcal{T}.
\end{aligned} \tag{7}$$

Formulas (6) and (7) for the Coulomb field correspond to the respective formulas from Ref. [26]. Omitting the contribution to vector $\mathbf{R}_x$ entering formula (6) from the term proportional to vector $\mathbf{Q}$ makes the integral over $\mathbf{Q}$ in Eqns (6) and (7) trivial and yields the Green's function calculated in the eikonal approximation [27]. Integration over x in this function corresponds to integration over the straight line along vector $\mathbf{r} = \mathbf{r}_2 - \mathbf{r}_1$. Accounting for the contribution from the term proportional to vector $\mathbf{Q}$ in $\mathbf{R}_x$ corresponds to that of quantum fluctuations in the plane perpendicular to vector $\mathbf{r}$.

Formulas for coefficients f_i ensue from Eqns (2)–(4), (6), and (7):

$$\begin{aligned}
f_0(\mathbf{r},\mathbf{p}) &= -\frac{\mathrm{i}}{\pi}\exp(-\mathrm{i}\mathbf{pr})\\
&\times\int \mathrm{d}\mathbf{Q}\left(1+\frac{\mathrm{i}}{2\varepsilon_p}\int_0^\infty \mathrm{d}x\int_0^x \mathrm{d}y\,(x-y)\boldsymbol{\nabla}_\perp V(\mathbf{r}_x)\boldsymbol{\nabla}_\perp V(\mathbf{r}_y)\right)\mathcal{T}_1\,,\\
\mathbf{f}_1(\mathbf{r},\mathbf{p}) &= \frac{1}{2\varepsilon_p}(\mathrm{i}\boldsymbol{\nabla}-\mathbf{p})f_0(\mathbf{r},\mathbf{p}) - \frac{\mathrm{i}}{4\pi\varepsilon_p^2}\exp(-\mathrm{i}\mathbf{pr})\\
&\quad\times\int \mathrm{d}\mathbf{Q}\int_0^\infty \mathrm{d}x\,\boldsymbol{\nabla}V^2(\mathbf{r}_x)\mathcal{T}_1\,,\\
\mathbf{f}_2(\mathbf{r},\mathbf{p}) &= -\frac{\exp(-\mathrm{i}\mathbf{pr})}{4\pi\varepsilon_p^2}\int \mathrm{d}\mathbf{Q}\int_0^\infty \mathrm{d}x\int_0^x \mathrm{d}y\,\big[\boldsymbol{\nabla}V(\mathbf{r}_x)\times\boldsymbol{\nabla}V(\mathbf{r}_y)\big]\mathcal{T}_1,\\
\mathcal{T}_1 &= \exp\left(\mathrm{i}Q^2 - \mathrm{i}\int_0^\infty \mathrm{d}x\,V(\mathbf{r}_x)\right), \quad \mathbf{r}_x = \mathbf{r} + x\mathbf{n}_{\mathbf{p}} + \mathbf{Q}\sqrt{\frac{2r}{\varepsilon_p}},
\end{aligned} \tag{8}$$

where $\mathbf{Q}\mathbf{n}_{\mathbf{p}} = 0$, $\boldsymbol{\nabla}_\perp$ is the gradient component normal to vector $\mathbf{n}_{\mathbf{p}} = \mathbf{p}/p$.

The formulas presented in this section are sufficient for calculating photoproduction and bremsstrahlung cross sections in the quasiclassical approximation taking account of the first-order quasiclassical correction.

3. Photoproduction of an e^+e^- pair

Production of an e^+e^- pair in an atomic field is one of the most important quantum electrodynamics (QED) processes for various applications [28, 29]. A large number of theoretical and experimental studies have dealt with this problem. The process cross section in the Born approximation is known for an arbitrary photon energy ω [2, 3]. The formal expression for the cross section exact in the parameter η and energy ω was derived in Ref. [5]. However, numerical results obtained with the use of this expression were reported only for $\omega < 12.5$ MeV [6] due to the difficulty of numerical calculations rapidly increasing with ω. Using the wave functions in the Furry–Sommerfeld–Maue approximation [10, 11], which are actually functions calculated in the leading quasiclassical approximation, made it possible to obtain in Refs [7, 8] simple expressions for Coulomb corrections in the leading approximation with respect to $m/\omega \ll 1$. However, these results are accurate enough only for very high energies: $\omega \gtrsim 100$ MeV.

The description of Coulomb corrections to the total photoproduction cross section at intermediate photon energies (5–100 MeV) has for a long time been based on the expression proposed in Ref. [30]. The expression is actually a formula for interpolation between the results obtained for $\omega < 5$ MeV and the high-energy asymptotics. Using the quasiclassical Green's function, the authors of paper [31] have found the first-order correction in m/ω to the electron spectrum and to the total cross section of the e^+e^- photoproduction process in a strong atomic field. A correction to the spectrum was obtained in the region where the two produced particles are relativistic. It proved to be antisymmetric with respect to $\varepsilon_p \leftrightarrow \varepsilon_q$ permutation, where ε_p and ε_q are electron and positron energies, respectively. For this reason, the correction to the total cross section is determined by the energy region close to the edge of the spectrum, where $\varepsilon_p \sim m$ or $\varepsilon_q \sim m$. In Ref. [31], a correction to the total cross section was found with the use of the dispersion relation for the amplitude of Delbrück forward scattering. Consideration of this correction has led to the agreement between predicted and experimental data for an intermediate photon energy. Correction to the spectrum for $\omega \gg m$ in the case of $\varepsilon_p \sim m$ or $\varepsilon_q \sim m$ was calculated in Ref. [32]. It turned out that Coulomb corrections at the edge of the spectrum are substantially different from those in the regions of $\varepsilon_p \gg m$ and $\varepsilon_q \gg m$. Integration of corrections to the spectrum found in Ref. [32] confirmed the result for corrections to the total cross section obtained in Ref. [31] with the use of the dispersion relation.

For many applications, it is important to know with a high degree of accuracy the differential photoproduction cross section for photon energies $\omega \lesssim 100$ MeV, for which the precision of results obtained in the leading quasiclassical approximation is insufficient. In Ref. [26], the differential cross section of photoproduction of electron–positron pairs was found exactly in η taking account of the first-order quasiclassical correction. The results of Ref. [26] in the region of $\omega \lesssim 100$ MeV are much more accurate than those calculated in the leading quasiclassical approximation.

For e^+e^--pair photoproduction, consideration of nuclear field screening by atomic electrons is important only for the Born contribution; its effect for Coulomb corrections is insignificant. At the same time, consideration of the difference between atomic and Coulomb fields at small distances (finite nucleus size effect) for e^+e^--pair photoproduction is of no consequence at all. For the photoproduction of a $\mu^+\mu^-$ pair, not only field screening but also the finite nucleus size must be taken into account. The calculation of the differential cross section of $\mu^+\mu^-$-pair photoproduction taking account of the first-order quasiclassical correction has recently been reported in Ref. [25].

3.1 Differential cross section of e^+e^--pair photoproduction

The differential cross section of e^+e^--pair photoproduction by a photon in an atomic field has the form

$$\begin{aligned} d\sigma(\mathbf{p},\mathbf{q},\eta) &= \frac{\alpha}{(2\pi)^4\omega}\, d\mathbf{p}\, d\mathbf{q}\, \delta(\omega-\varepsilon_p-\varepsilon_q)|M|^2\,, \\ M &= \int d\mathbf{r}\, \bar{u}^-_{\mathbf{p}}(\mathbf{r})\, \boldsymbol{\gamma}\, \mathbf{e}\, v^+_{\mathbf{q}}(\mathbf{r}) \exp(i\mathbf{k}\mathbf{r})\,. \end{aligned} \tag{9}$$

Here, $\mathbf{e}$ and $\mathbf{k}$ are the polarization vector and the photon momentum, respectively, and $\mathbf{p}$ and $\mathbf{q}$ are electron and positron momenta.

We further assume that summation over final particle polarizations and averaging over photon polarization are carried out in the differential cross section $d\sigma(\mathbf{p},\mathbf{q},\eta)$. This cross section can be represented as the sum of symmetric and asymmetric parts with respect to the permutation of $\mathbf{p}$ and $\mathbf{q}$ momenta:

$$\begin{aligned} d\sigma(\mathbf{p},\mathbf{q},\eta) &= d\sigma_s(\mathbf{p},\mathbf{q},\eta) + d\sigma_a(\mathbf{p},\mathbf{q},\eta)\,, \\ d\sigma_s(\mathbf{p},\mathbf{q},\eta) &= \frac{d\sigma(\mathbf{p},\mathbf{q},\eta)+d\sigma(\mathbf{q},\mathbf{p},\eta)}{2}\,, \\ d\sigma_a(\mathbf{p},\mathbf{q},\eta) &= \frac{d\sigma(\mathbf{p},\mathbf{q},\eta)-d\sigma(\mathbf{q},\mathbf{p},\eta)}{2}\,. \end{aligned} \tag{10}$$

Since the substitution of the electron by a positron corresponds to the change in the sign of η, then one has $d\sigma(\mathbf{p},\mathbf{q},\eta) = d\sigma(\mathbf{q},\mathbf{p},-\eta)$; therefore, $d\sigma_s(\mathbf{p},\mathbf{q},\eta)$ is the even function of η, while $d\sigma_a(\mathbf{p},\mathbf{q},\eta)$ is its odd function. The differential photoproduction cross section was found in the leading quasiclassical approximation in Refs [7, 8]. This cross section is the even function of η and makes a contribution only to $d\sigma_s(\mathbf{p},\mathbf{q},\eta)$. Hence, the following relations hold true:

$$\begin{aligned} d\sigma_s &= \frac{2\alpha m^2\left|\Gamma(1-i\eta)\right|^4 d\varepsilon_p\, d\boldsymbol{\delta}_p\, d\boldsymbol{\delta}_q}{\pi^2\omega^3\Delta^4} \\ &\quad\times\Big\{\left[(1-u)(\varepsilon_p^2+\varepsilon_q^2)+2\varepsilon_p\varepsilon_q(\xi_p-\xi_q)^2\right]\eta^2\mathcal{F}^2 \\ &\quad+\left[u(\varepsilon_p^2+\varepsilon_q^2)+2\varepsilon_p\varepsilon_q(1-\xi_p-\xi_q)^2\right](1-u)^2\mathcal{F}'^2\Big\}\,, \\ \mathcal{F} &= F(-i\eta, i\eta, 1, u)\,, \quad \mathcal{F}' = \frac{\partial\mathcal{F}}{\partial u}\,, \quad u = 1-\frac{\boldsymbol{\Delta}_\perp^2}{m^2}\,\xi_p\xi_q\,, \\ \xi_p &= \frac{1}{1+\delta_p^2}\,, \quad \xi_q = \frac{1}{1+\delta_q^2}\,, \\ \boldsymbol{\delta}_p &= \frac{\mathbf{p}_\perp}{m}\,, \quad \boldsymbol{\delta}_q = \frac{\mathbf{q}_\perp}{m}\,, \quad \boldsymbol{\Delta} = \mathbf{p}+\mathbf{q}-\mathbf{k}\,, \end{aligned} \tag{11}$$

where $F(a,b,c,x)$ is the hypergeometric function, $\Gamma(x)$ is Euler's gamma function, $\mathbf{p}_\perp$, $\mathbf{q}_\perp$, and $\boldsymbol{\Delta}_\perp$ are the components of vectors $\mathbf{p}$, $\mathbf{q}$, and $\boldsymbol{\Delta}$ normal to vector $\mathbf{k}$.

The quasiclassical correction to the photoproduction cross section found exactly in η in Ref. [26] is the odd function of η and makes a contribution only to $d\sigma_a(\mathbf{p},\mathbf{q},\eta)$, i.e., to the charge asymmetry in the photoproduction process:

$$\begin{aligned} d\sigma_a &= -\frac{\alpha m^2\eta^2\left|\Gamma(1-i\eta)\right|^2 d\varepsilon_p\, d\boldsymbol{\delta}_p\, d\boldsymbol{\delta}_q}{2\pi^{3/2}\omega^3\Delta^3} \\ &\quad\times \mathrm{Im}\left[\int_0^\infty \frac{d\lambda}{\sqrt{\lambda}}\left(\frac{1+\xi_p\lambda}{1+\xi_q\lambda}\right)^{i\eta}\frac{\sqrt{\xi_p}\,\Gamma(1-i\eta)\Gamma(1/2+i\eta)}{\varepsilon_q\sqrt{1+\xi_p\lambda}}\,\mathcal{M}\right. \\ &\quad\left.+(\mathbf{p}\leftrightarrow\mathbf{q}, \eta\to-\eta)\vphantom{\int_0^\infty}\right]\,, \\ \mathcal{M} &= \left[(\xi_p-\xi_q)\,i\eta\mathcal{F}+(1-\xi_p-\xi_q)\,(1-u)\mathcal{F}'\right] \\ &\quad\times\left[4\varepsilon_p\varepsilon_q(\xi_p f_1+\xi_q f_2+f_3)+(\varepsilon_p^2+\varepsilon_q^2)(f_1+f_2+2f_3)\right] \\ &\quad+(\varepsilon_p^2+\varepsilon_q^2)(1-u)\left[(f_1-f_2)\,i\eta\mathcal{F}-u(f_1+f_2)\mathcal{F}'\right]\,, \\ f_1 &= \frac{(1/2-i\eta)\mathcal{G}-(1-z)\mathcal{G}'}{1+\xi_p\lambda}\,, \quad f_2 = \frac{i\eta\mathcal{G}-(1-z)\mathcal{G}'}{1+\xi_q\lambda}\,, \\ f_3 &= \frac{(1-z)\mathcal{G}'}{1+\lambda}\,, \quad \mathcal{G} = F\left(\frac{1}{2}-i\eta,\, i\eta, 1, z\right)\,, \quad \mathcal{G}' = \frac{\partial\mathcal{G}}{\partial z}\,, \\ z &= 1-\frac{\Delta^2\xi_p\xi_q(1+\lambda)}{m^2(1+\xi_p\lambda)(1+\xi_q\lambda)}\,. \end{aligned} \tag{12}$$

As it must be, the correction $d\sigma_a$ is invariant with respect to the $\mathbf{p}\leftrightarrow\mathbf{q}$, $\eta\to-\eta$ substitutions. Because i enters the expression for $d\sigma_a$ only in the $i\eta$ combination, the quantity $d\sigma_a$ is obviously antisymmetric with respect to the $\eta\to-\eta$ and $\mathbf{p}\leftrightarrow\mathbf{q}$ substitutions.

To take account of the field screening, it suffices to multiply $d\sigma_s$ (11) by $|F(\Delta^2)|^2$, where $F(\Delta^2)$ is the atomic form factor, because Coulomb corrections are of significance only in the region of $\Delta \gtrsim m$, where $F(\Delta^2)\approx 1$. This means that the atomic form factor influences only the Born cross section at small $\Delta \sim r_{scr}^{-1} \ll m$, where r_{scr} is the screening radius: $r_{scr} \sim Z^{-1/3}/(m\alpha)$. Expansion of $d\sigma_a(\mathbf{p},\mathbf{q},\eta)$ into a series of η starts from the terms proportional to η^3; therefore,

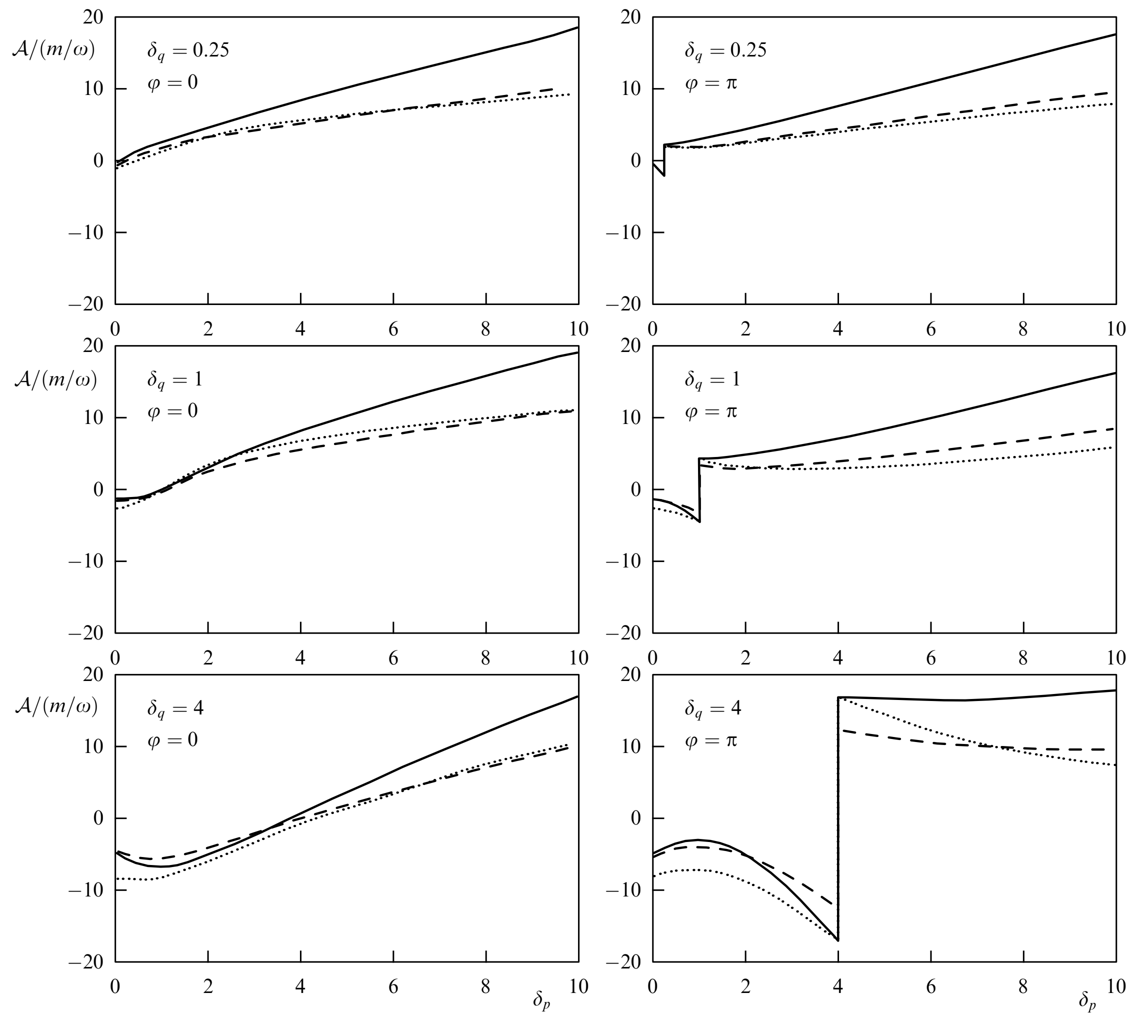

Figure 1. Dependence of $\mathcal{A}$ (in units of m/ω) on δ_p for a few values of δ_q, φ, and $x = \varepsilon_p/\omega$: $x = 0.25$ (solid curve), $x = 0.5$ (dashed curve), and $x = 0.75$ (dotted curve); $\eta = 0.54$ (tungsten).

the value of $\mathrm{d}\sigma_{\mathrm{a}}(\mathbf{p}, \mathbf{q}, \eta)$ totally depends on the Coulomb corrections and is insensitive to screening. For this reason, the formula for $\mathrm{d}\sigma_{\mathrm{a}}(\mathbf{p}, \mathbf{q}, \eta)$ derived in the Coulomb field holds true for the atomic field, too.

Charge asymmetry $\mathcal{A}$ in the differential photoproduction cross section is given by the ratio

$$\mathcal{A} = \frac{\mathrm{d}\sigma_{\mathrm{a}}(\mathbf{p}, \mathbf{q}, \eta)}{\mathrm{d}\sigma_{\mathrm{s}}(\mathbf{p}, \mathbf{q}, \eta)} \,. \tag{13}$$

Outside a very narrow region, $\Delta_\perp \lesssim |\Delta_\parallel| = |\mathbf{k}\boldsymbol{\Delta}|/\omega \sim m^2/\omega$, it is possible to make the substitution $\Delta^2 \to \boldsymbol{\Delta}_\perp^2 = m^2(\boldsymbol{\delta}_p + \boldsymbol{\delta}_q)^2$. Therefore [as follows from Eqns (11) and (12)], asymmetry $\mathcal{A}$ at fixed values of $\boldsymbol{\delta}_p$, $\boldsymbol{\delta}_q$, and $x = \varepsilon_p/\omega$ is inversely proportional to ω. Figure 1 plots the dependence of $\mathcal{A}$ on δ_p for tungsten ($\eta = 0.54$) at several δ_q and φ values, where φ is the angle between vectors $\boldsymbol{\delta}_p$ and $\boldsymbol{\delta}_q$. It can be seen that the charge asymmetry can be large enough ($\mathcal{A} \sim 20-30\%$ at $\omega/m = 50$). It increases when δ_p and/or δ_q become greater than unity.

At $\varphi = \pi$, there is a jump in asymmetry $\mathcal{A}$ at the point $\delta_p = \delta_q$, where $|\boldsymbol{\Delta}_\perp| = 0$. At this point, $\mathcal{A}$ changes its sign. Notice that the screening needs to be taken into account in $\mathcal{A}$ only in a very narrow region of $|\boldsymbol{\Delta}_\perp| \lesssim r_{\mathrm{scr}}^{-1}$.

The importance of contributions from higher-order terms in η to asymmetry is illustrated in Fig. 2, presenting the dependence of $\mathcal{A}$ on $\eta = Z\alpha$ at $\delta_p = 2$, $\delta_q = 4$ and a few values of $x = \varepsilon_p/\omega$ and φ. The dashed curve was obtained in the leading approximation in η (linear in η). Evidently, the η dependence of $\mathcal{A}$ is rather strong even at intermediate η values.

Let us consider the photoproduction cross section integrated over positron emission angles (over $\boldsymbol{\delta}_q$). Direct integration of formula (12) encounters difficulty. However, we can take advantage of the fact that a recount from the corresponding bremsstrahlung cross section is valid for such an integrated cross section. The use of formula (56) from Section 4 leads to the following relations

$$\begin{aligned}
\frac{\mathrm{d}\sigma_{\mathrm{s}}}{\mathrm{d}\mathbf{p}} &= \frac{4\alpha\eta^2\xi_p^2}{\pi m^4\omega^3}\left\{(\varepsilon_p^2+\varepsilon_q^2)L + \varepsilon_p\varepsilon_q\left[1+4\xi_p(1-\xi_p)\left(L-\frac{3}{2}\right)\right]\right\},\\
\frac{\mathrm{d}\sigma_{\mathrm{a}}}{\mathrm{d}\mathbf{p}} &= \frac{\pi\alpha\eta^2\,\mathrm{Re}\,g(\eta)}{m^3\omega^3\varepsilon_p\varepsilon_q}\,\xi_p\big[\varepsilon_q(\varepsilon_p^2+\varepsilon_q^2+2\varepsilon_p\omega\xi_p)F_1\\
&\quad - \xi_p(\varepsilon_p^2\omega + \varepsilon_q^3 + 4\varepsilon_p\varepsilon_q\omega\xi_p)F_2\big]\,,\\
L &= \ln\left(\frac{2\varepsilon_p\varepsilon_q}{m\omega}\right) - \frac{1}{2} - f(\eta)\,,\\
F_1 &= F\left(\frac{1}{2},\frac{1}{2}\,;\,1;\,-\delta_p^2\right) = \frac{2}{\pi}\,K(-\delta_p^2)\,,\\
F_2 &= F\left(-\frac{1}{2},\frac{1}{2}\,;\,1;\,-\delta_p^2\right) = \frac{2}{\pi}\,E(-\delta_p^2)\,,
\end{aligned} \tag{14}$$

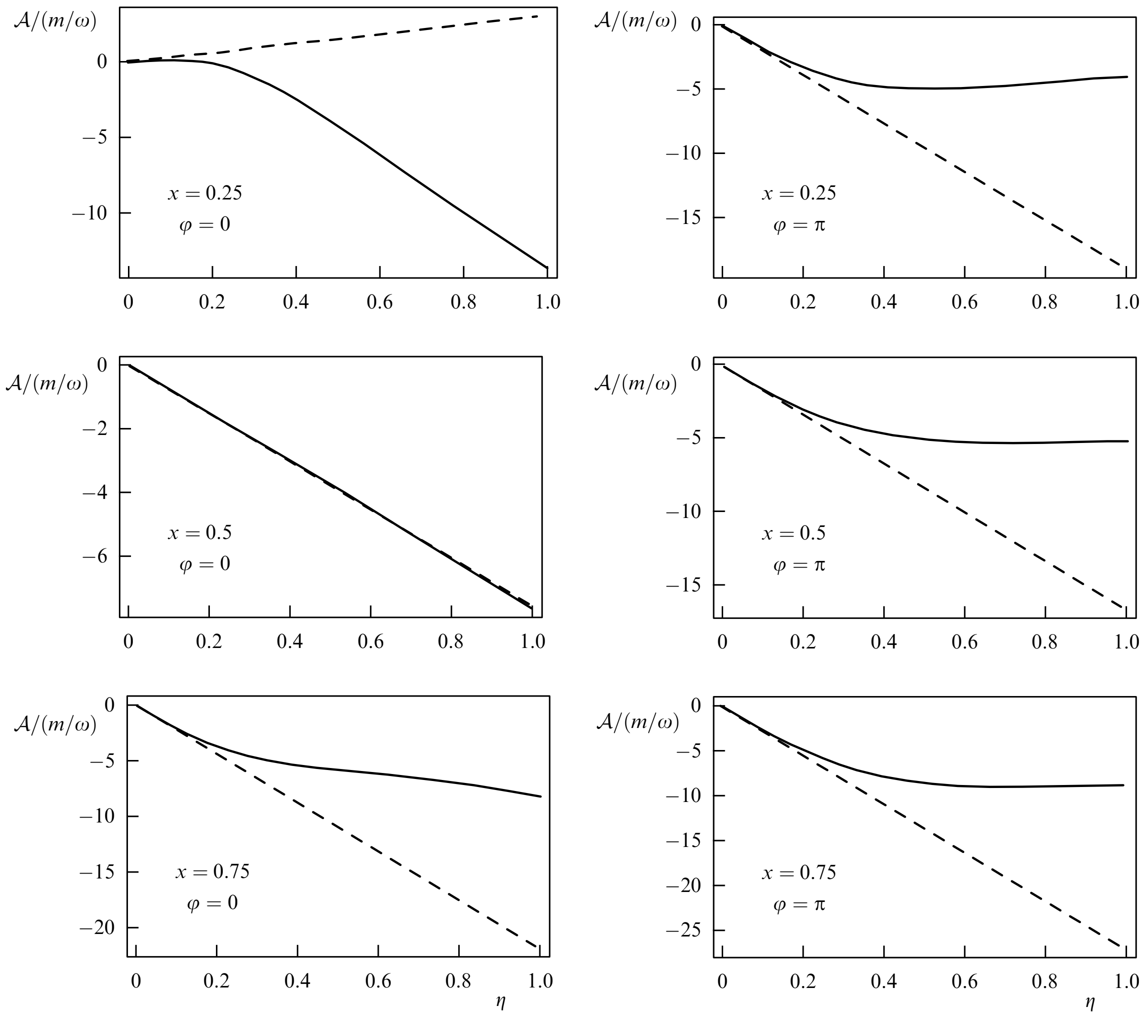

Figure 2. Dependence of $\mathcal{A}$ (in units of m/ω) on $\eta = Z\alpha$ at $\delta_p = 2$, $\delta_q = 4$, and for a few values of x and φ. Solid curve — the result exact in η. The dashed curve is obtained in the leading approximation in η (linear in η).

where K and E are the elliptic functions. Functions f and g in Eqn (14) are expressed through the Euler gamma function $\Gamma(t)$ and its logarithmic derivative $\psi(t) = \mathrm{d}\ln\Gamma(t)/\mathrm{d}t$:

$$f(\eta) = \mathrm{Re}\left[\psi(1+\mathrm{i}\eta) - \psi(1)\right],$$
$$g(\eta) = \eta\,\frac{\Gamma(1-\mathrm{i}\eta)\,\Gamma(1/2+\mathrm{i}\eta)}{\Gamma(1+\mathrm{i}\eta)\,\Gamma(1/2-\mathrm{i}\eta)}\,. \qquad (15)$$

Expression (14) holds true for the case of a Coulomb field. The influence of field screening on the Born contribution is well known; it reduces to a change of the logarithm argument and the constant in L (see Ref. [12]). The influence of screening on Coulomb corrections can be neglected.

Charge asymmetry $\mathcal{A}_1$ is defined by the following formula

$$\mathcal{A}_1 = \frac{\mathrm{d}\sigma_\mathrm{a}/\mathrm{d}\mathbf{p}}{\mathrm{d}\sigma_\mathrm{s}/\mathrm{d}\mathbf{p}}\,. \qquad (16)$$

Figure 3 depicts the dependence of $\mathcal{A}_1$ on δ_p at $\eta = 0.54$ (tungsten), $\omega/m = 50$, and for several x values. The ω dependence of $\mathcal{A}_1$, unlike the $\mathcal{A}(\omega)$ dependence, is not reduced to the m/ω factor due to the logarithmic dependence of $\mathrm{d}\sigma_\mathrm{s}(\mathbf{p},\eta)$ on ω. Evidently, the charge asymmetry $\mathcal{A}_1$ is noticeable, even if it is much weaker than asymmetry $\mathcal{A}$.

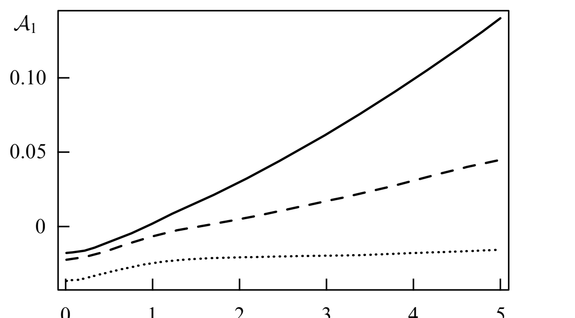

Figure 3. Dependence of $\mathcal{A}_1$ on δ_p at $x = 0.25$ (solid curve), $x = 0.5$ (dashed curve), and $x = 0.75$ (dotted curve); $\eta = 0.54$ (tungsten), and $\omega/m = 50$.

3.2 Differential cross section of $\mu^+\mu^-$-pair photoproduction

Photoproduction of a $\mu^+\mu^-$ pair off heavy atoms is an equally important QED process. Calculation of the photoproduction cross section for muons requires, unlike that for the e^+e^- pair, taking into account the finiteness of nuclear size R (the difference between the nuclear field and the Coulomb field for distances $r < R$). The Born cross section is proportional to the square of the nuclear form factor $F_n(\Delta^2)$ and sensitive to its shape, because the muon Compton wavelength for heavy nuclei $\lambda_\mu = 1/m_\mu = 1.87$ fm (m_μ is the muon mass) is shorter than the nucleus radius ($R = 7.3$ fm for gold, and $R = 7.2$ fm for lead). Coulomb corrections to the total cross section of muon pair photoproduction were discussed in Refs [33–35]. Unlike the main contribution to the total Born cross section determined by impact parameters ρ in the $R \ll \rho \ll \omega^2/m$ region, the main contribution to Coulomb corrections to the total cross section is determined by impact parameters within the $\rho \sim \lambda_\mu \lesssim R$ range. As a result, Coulomb corrections to the total cross section are strongly suppressed by the nuclear form factor. It had been supposed for a long time that this assertion was true for all quantities related to Coulomb corrections. However, a recent study of charge asymmetry in the differential cross section of $\mu^+\mu^-$-pair photoproduction (see Ref. [25]) for $\omega \gg m_\mu$ refuted it.

For momentum transfer $\Delta_\perp \gtrsim 1/R$, taking account of the form factor results in strong suppression of the cross section; here, $\mathbf{\Delta} = \mathbf{p} + \mathbf{q} - \mathbf{k}$, $\mathbf{p}$ is the μ^- momentum, and $\mathbf{q}$ is the μ^+ momentum. Therefore, charge asymmetry is quite apparent in the $\Delta_\perp \lesssim 1/R$ region at $p_\perp \sim q_\perp \sim m \gg \Delta_\perp$, so that $|\mathbf{p}_\perp + \mathbf{q}_\perp| \ll |\mathbf{p}_\perp - \mathbf{q}_\perp|$. It was shown in Ref. [26] that in this region only the contribution proportional to η^3 (even at $\eta \sim 1$) remains in the expansion of Coulomb corrections in terms of η. The contribution to the $d\sigma_a(\mathbf{p}, \mathbf{q}, \eta)$ cross section proportional to η^3 in the $|\mathbf{p}_\perp + \mathbf{q}_\perp| \ll |\mathbf{p}_\perp - \mathbf{q}_\perp|$ region taking account of the nucleus form factor was calculated in Ref. [25]. This contribution determines charge asymmetry $\mathcal{A} \propto \eta$. In this region, both quantities, $\mathcal{A}$ and $d\sigma_s(\mathbf{p}, \mathbf{q}, \eta) \propto \eta^2$, were shown to be large enough to be observed in experiment. The $d\sigma_a$ cross section for $p_\perp \gg m$ and $q_\perp \gg m$ was studied in Ref. [36] for the photoproduction of a pair of scalar particles.

For photoproduction of a $\mu^+\mu^-$ pair, the leading in η contribution to the cross section $d\sigma_s$ has the form [4]

$$d\sigma_s = \frac{2\alpha m^2\, d\varepsilon_p\, d\boldsymbol{\delta}_p\, d\boldsymbol{\delta}_q}{(2\pi)^4\omega^3}\, V_F^2(\Delta^2) \times \left[\frac{\Delta^2}{m^2}\,\xi_p\xi_q(\varepsilon_p^2 + \varepsilon_q^2) + 2\varepsilon_p\varepsilon_q(\xi_p - \xi_q)^2\right], \tag{17}$$

where $V_F(\Delta^2) = -4\pi\eta F_n(\Delta^2)/\Delta^2$, $F_n(\Delta^2)$ is the nucleus form factor significantly different from unity for $\Delta \gtrsim 1/R$ [see formula (11) for other notations]. The following result was obtained in Ref. [36] for the antisymmetric part of the cross section:

$$d\sigma_a = \frac{\alpha m^2\, d\varepsilon_p\, d\boldsymbol{\delta}_p\, d\boldsymbol{\delta}_q}{(2\pi)^4\omega^3}\left\{(\xi_p - \xi_q)\left[4(\varepsilon_p\xi_p + \varepsilon_q\xi_q) + \frac{\omega(\varepsilon_p^2 + \varepsilon_q^2)}{\varepsilon_p\varepsilon_q}\right] + (\varepsilon_p - \varepsilon_q)\,\frac{\varepsilon_p^2 + \varepsilon_q^2}{\varepsilon_p\varepsilon_q}\,\frac{\Delta^2}{m^2}\,\xi_p\xi_q\right\} V_F(\Delta^2)J(\Delta)\,, \tag{18}$$

where

$$J(\Delta) = \int \frac{d\mathbf{s}}{(2\pi)^3}\left[V_F(Q_+)V_F(Q_-) + (\Delta^2 - 4s_\parallel^2)V_F(Q_+)V_F'(Q_-)\right], \tag{19}$$

$$Q_\pm = \left(\mathbf{s} \pm \frac{\mathbf{\Delta}}{2}\right)^2, \quad s_\parallel = \mathbf{s}\,\frac{\mathbf{\Delta}}{\Delta}\,, \quad V_F'(Q) = \frac{\partial V_F(Q)}{\partial Q}\,. \tag{20}$$

For the Coulomb field, one finds $J(\Delta) = 2\pi^2\eta^2/\Delta$. In the formula for charge asymmetry, $\mathcal{A} = d\sigma_a/d\sigma_s$, the entire dependence on the nuclear charge is contained in the $J(\Delta)/V_F(\Delta^2)$ ratio. The nucleus form factor is fairly well approximated by the function

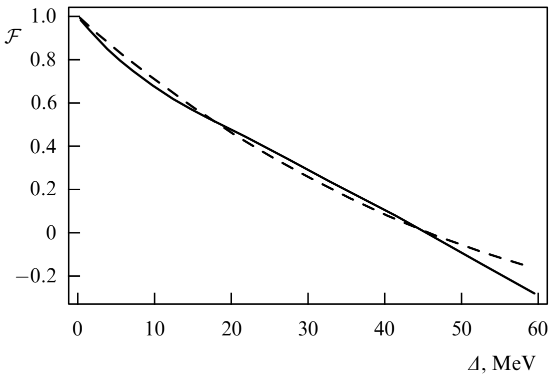

Figure 4. Dependence of function $\mathcal{F}(\Delta)$ on Δ for lead ($Z = 82$). Solid curve correspond to the real charge distribution. Dashed curve was calculated by formula (22) with $\Lambda = 60$ MeV.

$$F_n(\Delta^2) = \frac{\Lambda^2}{\Delta^2 + \Lambda^2}\,, \tag{21}$$

where $\Lambda \sim 60$ MeV for heavy nuclei. In this case, function $\mathcal{F}(\Delta) = -2J(\Delta)/(\pi\eta\Delta V_F(\Delta^2))$ takes the simple form

$$\mathcal{F}(\Delta) = \left(1 + \frac{\Delta^2}{\Lambda^2}\right)\left[1 + \frac{2}{\pi}\arctan\left(\frac{\Delta}{2\Lambda}\right) - \frac{4}{\pi}\arctan\left(\frac{\Delta}{\Lambda}\right)\right] - \frac{12\Delta\Lambda}{\pi(\Delta^2 + 4\Lambda^2)}\,. \tag{22}$$

For $\Delta \ll \Lambda$, there is the asymptotics $\mathcal{F}(\Delta) \approx 1 - 6\Delta/(\pi\Lambda)$, and function $\mathcal{F}(\Delta)$ rapidly decreases with increasing Δ. Figure 4 shows the dependence of $\mathcal{F}(\Delta)$ on Δ for lead ($Z = 82$).

For $\Delta \ll |\mathbf{p}_\perp - \mathbf{q}_\perp|$, formula (18) is simplified to

$$d\sigma_a = \frac{\alpha m^2\, d\varepsilon_p\, d\boldsymbol{\delta}_p\, d\boldsymbol{\delta}_q}{(2\pi)^4\omega^2}\,(\xi_p - \xi_q) \times \left[2(\xi_p + \xi_q) + \frac{\varepsilon_p^2 + \varepsilon_q^2}{\varepsilon_p\varepsilon_q}\right] V_F(\Delta^2)J(\Delta)\,. \tag{23}$$

Hence, for charge asymmetry $\mathcal{A}$ one has the expression

$$\mathcal{A} = \frac{\pi\eta m\omega\kappa(\xi_p + \xi_q + B)}{4\varepsilon_p\varepsilon_q(B + \kappa^2\xi_p\xi_q)}\,\mathcal{F}(\Delta)\,, \quad B = \frac{\varepsilon_p^2 + \varepsilon_q^2}{2\varepsilon_p\varepsilon_q}\,, \quad \kappa = \frac{m(\xi_q - \xi_p)}{\Delta\xi_p\xi_q}\,. \tag{24}$$

To find out the characteristic value of asymmetry $\mathcal{A}$, we consider the region interesting from the experimental standpoint: $|\phi| \ll |\varepsilon_p - \varepsilon_q|/\omega \ll 1$ and $|\theta_p - \theta_q|/|\theta_p + \theta_q| \ll |\varepsilon_p - \varepsilon_q|/\omega$, where ϕ is the angle between vectors $\mathbf{p}_\perp$ and $-\mathbf{q}_\perp$. In this region, one finds

$$\mathcal{A} = \frac{\pi\eta\theta(1 + 2\xi)}{(1 + 4\xi^2\delta^2)}\,\mathcal{F}\big(\theta|\varepsilon_p - \varepsilon_q|\big)\,\mathrm{sgn}\,(\varepsilon_p - \varepsilon_q)\,, \quad \theta = \frac{1}{2}(\theta_p + \theta_q), \quad \delta = \frac{\omega\theta}{2m}\,, \quad \xi = \frac{1}{1 + \delta^2}\,, \tag{25}$$

and the entire dependence on $\varepsilon_p - \varepsilon_q$ is contained in the function $\mathcal{F}$. Since Eqn (24) holds for all $\eta \lesssim 1$, the factor in front of $\mathcal{F}$ in Eqn (25) may be well above 10%.

3.3 Electron spectrum in the process of e^+e^--pair photoproduction

To obtain the photoproduction spectrum in the $\varepsilon_{p,q} \gg m$ region, it suffices to integrate the expressions for $d\sigma_s$ and $d\sigma_a$ from Eqn (14) over electron emission angles. The result is as follows:

$$\frac{d\sigma_s}{dx} = 4\sigma_0\left[1 - \frac{4}{3}\,x(1-x)\right]L\,,$$
$$\frac{d\sigma_a}{dx} = \frac{\sigma_0\pi^3(1-2x)m}{2x(1-x)\omega}\left[1 - \frac{3}{2}\,x(1-x)\right]\mathrm{Re}\,g(\eta)\,, \qquad (26)$$

where L and $g(\eta)$ are given in formulas (14) and (15), respectively, $x = \varepsilon_p/\omega$ is the fraction of electron energy, and $\sigma_0 = \alpha\eta^2/m^2$. The sum $d\sigma_s/dx + d\sigma_a/dx$ defines the spectrum of the photoproduction process calculated in the quasiclassical approximation taking into consideration the first-order quasiclassical correction. To obtain the expression for Coulomb corrections to the spectrum, $d\sigma_C/dx$, it suffices to substitute the function $-f(\eta)$ for L in $d\sigma_s/dx$ and leave $d\sigma_a/dx$ unaltered. Formula (26), similar to formula (14), holds true for the Coulomb field, but the field screening effect is essential only in the Born contribution. The influence of screening on Coulomb corrections reduces to a contribution small in parameter $1/(mr_{\rm scr})$ [8]. The quantitative consideration of the screening effect on Coulomb corrections is reported in Ref. [26]. It is worthwhile to note that Coulomb corrections to the spectrum were found in Ref. [31] before the calculation of differential cross section and that integrated over a single particle. The $d\sigma_a/dx$ contribution increases the probability of electron production for $x < 1/2$, and decreases it for $x > 1/2$. Evidently, the opposite situation takes place for positrons. This property of the spectrum manifests itself at any ω and is most pronounced at low photon energies, $\omega > 2m$ [5]. For intermediate ω, spectrum (26) is substantially different from that calculated in the leading quasiclassical approximation. This inference is illustrated in Fig. 5 showing $\sigma_0^{-1}\,d\sigma_C/dx$ with (solid curve) and without (dashed curve) correction for lead ($Z = 82$) at $\omega = 50$ MeV.

3.4 Coulomb corrections to the total photoproduction cross section

The Coulomb correction to the total cross section of photoproduction in the Coulomb field was calculated in the leading quasiclassical approximation in paper [8]:

$$\sigma_C^{(0)} = -\frac{28}{9}\,\sigma_0 f(\eta)\,. \qquad (27)$$

It was shown [26] that a change of the Coulomb corrections to the total cross section, resulting from an allowance for screening, is fairly well approximated by the formula

$$\sigma_C^{\rm scr} \approx -5.4\times10^{-4}\,Z\sigma_C^{(0)}\,. \qquad (28)$$

Due to charge antisymmetry of $d\sigma_C^{(1)}/dx$ for $\varepsilon_{p,q} \gg m$, the contribution $\sigma_C^{(1)}$ to the total cross section may come only from the energy region $\varepsilon_p \sim m$ or $\varepsilon_q = \omega - \varepsilon_p \sim m$. The quasiclassical approximation is inapplicable in these regions, and a different approach is needed to calculate the spectrum (see Section 3.5).

Nonetheless, the correction to total cross section might be evaluated with the use of the quasiclassical approximation alone. For this purpose, the optical theorem was applied in paper [31], which links the imaginary part of the Delbrück forward scattering amplitude M_D (i.e., photon scattering in an atomic field through the production and subsequent annihilation of a virtual electron–positron pair [24]) with the sum of photoproduction cross sections for a continuous spectrum electron and a bound-state electron ($\sigma_{\rm coh}$ and $\sigma_{\rm bf}$, respectively):

$$\frac{1}{\omega}\,\mathrm{Im}\,M_D = \sigma_{\rm coh} + \sigma_{\rm bf}\,. \qquad (29)$$

In accordance with the Pauli exclusion principle, production of an e^+e^- pair by a photon on a neutral atom is not associated with the production of an electron in the bound state. Nevertheless, term $\sigma_{\rm bf}$ should be taken into consideration in the right-hand side of Eqn (29). The total photoproduction cross section $\sigma_{\rm bf}$ in the Coulomb field was found in paper [37] for $\omega \gg m$. In this limit, $\sigma_{\rm bf}$ is inversely proportional to ω and must be taken into account when relation (29) is used in calculating corrections to $\sigma_{\rm coh}$. The main contribution to $\sigma_{\rm bf}$ for $\omega \gg m$ comes from electrons in the low-lying bound states for which screening can be neglected. Due to this, the cross section $\sigma_{\rm bf}$ obtained in Ref. [37] can be used in formula (29) in the following form [37]

$$\sigma_{\rm bf} = 4\pi\sigma_0\eta^3\,h(\eta)\,\frac{m}{\omega}\,; \qquad (30)$$

function $h(\eta)$ is plotted in Fig. 6.

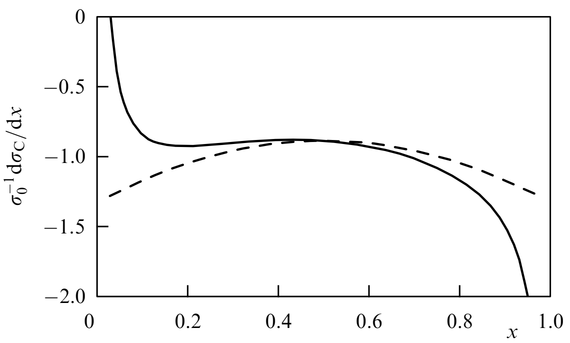

Figure 5. Dependence of $\sigma_0^{-1}\,d\sigma_C/dx$ on x (26) for lead ($Z = 82$) at $\omega = 50$ MeV. Dashed curve — the main contribution, and solid curve — the contribution taking account of the first-order quasiclassical correction.

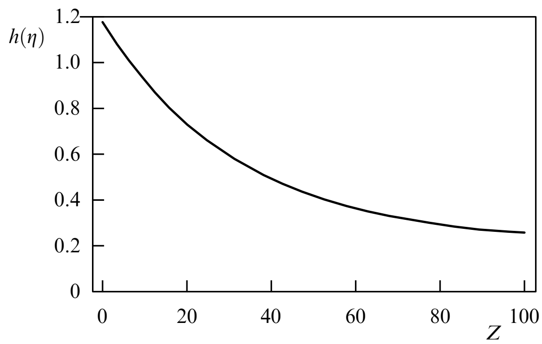

Figure 6. Dependence of the function $h(\eta)$ on Z, with $\eta = Z\alpha$.

The leading quasiclassical contribution to Coulomb corrections to the Delbrück forward scattering amplitude ensues from formulas (27) and (29):

$$M_{\mathrm{DC}}^{(0)} = -\mathrm{i}\,\frac{28}{9}\,\omega\sigma_0 f(\eta)\,. \tag{31}$$

The real part of the first-order correction $M_{\mathrm{DC}}^{(1)}$ in m/ω can just as well be calculated in the framework of the quasiclassical approximation [31]:

$$\mathrm{Re}\,M_{\mathrm{DC}}^{(1)} = \frac{\alpha\eta^2\pi^3\,\mathrm{Im}\,g(\eta)}{m}\,\ln\frac{\omega}{m}\,. \tag{32}$$

The large value of logarithm, $\ln(\omega/m)$, appears due to integration over a virtual electron energy ε in the region $\delta < \varepsilon < \omega - \delta$, where $\omega \gg \delta \gg m$. Just this makes possible the use of the quasiclassical approximation for calculating $\mathrm{Re}\,M_{\mathrm{DC}}^{(1)}$. The imaginary part of $M_{\mathrm{DC}}^{(1)}$ does not contain $\ln(\omega/m)$ and is determined by integration domains $\varepsilon \sim m$ and $\omega - \varepsilon \sim m$, in which the quasiclassical approximation proves to be inapplicable. Nevertheless, the $\mathrm{Im}\,M_{\mathrm{DC}}^{(1)}$ quantity associated with $\sigma_{\mathrm{C}}^{(1)}$ (29) can be obtained from the dispersion relation for M_{D} [38]:

$$\mathrm{Re}\,M_{\mathrm{D}}(\omega) = \frac{2}{\pi}\,\omega^2\,\mathrm{P}\int_0^\infty \frac{\mathrm{Im}\,M_{\mathrm{D}}(\omega')\,\mathrm{d}\omega'}{\omega'(\omega'^2-\omega^2)}\,, \tag{33}$$

where P denotes integration in a principal value sense. It follows from this equation that high-energy asymptotics of $\mathrm{Re}\,M_{\mathrm{DC}}^{(1)}$ (32) is unambiguously related to high-energy asymptotics of $\mathrm{Im}\,M_{\mathrm{DC}}^{(1)}$:

$$\mathrm{Im}\,M_{\mathrm{DC}}^{(1)} = -\frac{\alpha\eta^2\pi^4\,\mathrm{Im}\,g(\eta)}{2m}\,. \tag{34}$$

As a result, the following expression for correction $\sigma_{\mathrm{C}}^{(1)}$ ensues from the optical theorem (29):

$$\sigma_{\mathrm{C}}^{(1)} = \sigma_0\left(-\frac{\pi^4}{2}\,\mathrm{Im}\,g(\eta) - 4\pi\eta^3\,h(\eta)\right)\frac{m}{\omega}\,. \tag{35}$$

The quantity $(\omega/m)\sigma_{\mathrm{C}}^{(1)}/\sigma_{\mathrm{C}}^{(0)}$ is plotted in Fig. 7 by the solid curve. It can be seen that this ratio is high for any Z. Therefore, $\sigma_{\mathrm{C}}^{(1)}$ makes an appreciable contribution to the Coulomb corrections σ_{C} to the total photoproduction cross section at intermediate photon energies. The dashed curve in Fig. 7 corresponds to the same ratio if σ_{bf} in Eqn (35) is disregarded. Evidently, the relative contribution of the term in formula (35) proportional to $h(\eta)$ is numerically small.

It follows from the arguments offered in paper [8] that Coulomb corrections σ_{C} to the total photoproduction cross section in the Coulomb field can be presented in the form of the expansion

$$\sigma_{\mathrm{C}} = \sigma_{\mathrm{C}}^{(0)} + \sigma_{\mathrm{C}}^{(1)} + \sigma_{\mathrm{C}}^{(2)} + \ldots\,. \tag{36}$$

The term $\sigma_{\mathrm{C}}^{(n)}$ has the form $(m/\omega)^n L^{(n)}(\ln(\omega/m))$, where $L^{(n)}(x)$ is a certain polynomial. The ω-independent term $\sigma_{\mathrm{C}}^{(0)}$ corresponds to the result obtained in paper [8]. It follows from expression (35) for $\sigma_{\mathrm{C}}^{(1)}$ that coefficient $L^{(1)}$ is unrelated to ω, in conflict with the assumption that $L^{(1)}(x)$ is a second-degree polynomial (see Ref. [30]). The most accurate experimental

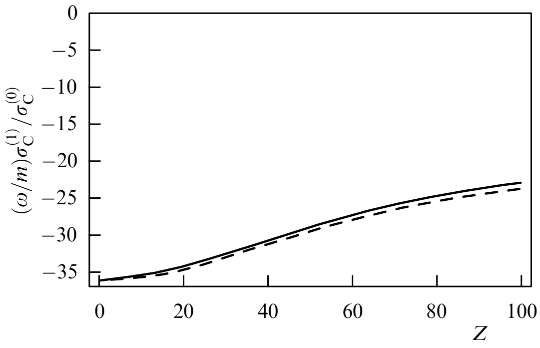

Figure 7. Ratio $(\omega/m)\sigma_{\mathrm{C}}^{(1)}/\sigma_{\mathrm{C}}^{(0)}$ as a function of Z (solid curve). The dashed curve corresponds to the same ratio calculated without regard for electron production in the bound state.

data for the photoproduction cross section have been obtained for intermediate photon energies [39–41]. In this region, correction $\sigma_{\mathrm{C}}^{(1)}$ is large (see Fig. 7) and the next-to-leading-order correction $\sigma_{\mathrm{C}}^{(2)}$ in expansion (36) can be substantial as well. Parametrization in the form

$$\sigma_{\mathrm{C}}^{(2)} = \sigma_0\left(b\ln\frac{\omega}{2m} + c\right)\left(\frac{m}{\omega}\right)^2, \tag{37}$$

where b and c are certain functions of η, was used for this correction in Ref. [31]. Experimental data for σ_{coh} are fairly well described by the formula

$$\sigma_{\mathrm{coh}} = \sigma_{\mathrm{B}} + \sigma_{\mathrm{C}}^{(0)} + \sigma_{\mathrm{C}}^{\mathrm{scr}} + \sigma_{\mathrm{C}}^{(1)} + \sigma_{\mathrm{C}}^{(2)}\,, \tag{38}$$

where σ_{B} is the Born cross section [4], $\sigma_{\mathrm{C}}^{(0)}$, $\sigma_{\mathrm{C}}^{\mathrm{scr}}$, and $\sigma_{\mathrm{C}}^{(1)}$ are given by formulas (27), (28), and (35), $\sigma_{\mathrm{C}}^{(2)}$ is defined in formula (37) with $b = 3.78\,(\omega/m)\,\sigma_0^{-1}\sigma_{\mathrm{C}}^{(1)}$, and $c = 0$.

Figure 8 shows the $S = (\sigma_{\mathrm{coh}} - \sigma_{\mathrm{B}})/\sigma_{\mathrm{C}}^{(0)}$ ratio presenting a Coulomb correction in units of $\sigma_{\mathrm{C}}^{(0)}$ (27).

The results obtained in Ref. [31] are shown by the solid curve, and theoretical predictions [30] by the dashed curve. Experimental data for S are borrowed from Ref. [39] for bismuth, and from Refs [40, 41] for lead. Evidently, the results of study [31] are in excellent agreement with experiment. The difference between the results reported in Refs [30] and [31] is insignificant at relatively low energies and becomes appreciable as the energies increase. This difference tends toward constant $\sigma_{\mathrm{C}}^{\mathrm{scr}}/\sigma_{\mathrm{C}}^{(0)}$ as $\omega \to \infty$, i.e., it arises from disregarding the effect of screening on Coulomb corrections in Ref. [30].

3.5 Photoproduction of an e^+e^- pair at $\varepsilon_p \sim m$ or $\varepsilon_q \sim m$

The photoproduction cross section at the edge of the spectrum ($\varepsilon_p \sim m$ or $\varepsilon_q \sim m$) was studied in Refs [32, 42]. Paper [42] examined the distribution over angles θ between positron ($\mathbf{q}$) and photon ($\mathbf{k}$) momenta at electron energies ε_p much lower than positron energy ε_q; under these conditions, the electron was not necessarily ultrarelativistic. Moreover, it was assumed that the condition $\sqrt{\varepsilon_p/\omega} \gg \theta \gg \varepsilon_p/\omega$ was fulfilled, which implied a large transverse positron momentum $\varDelta = \varepsilon_q\theta \gg \varepsilon_p$ but a small θ angle. In this region, the Born cross section integrated over electron emission angles has the form [4]

$$\frac{\mathrm{d}\sigma_{\mathrm{B}}}{\mathrm{d}\mathbf{q}} = \frac{2\alpha\eta^2}{\pi\omega\varDelta^4}\,\ln\left(\frac{1+\beta_p}{1-\beta_p}\right), \qquad \beta_p = \frac{p}{\varepsilon_p}\,. \tag{39}$$

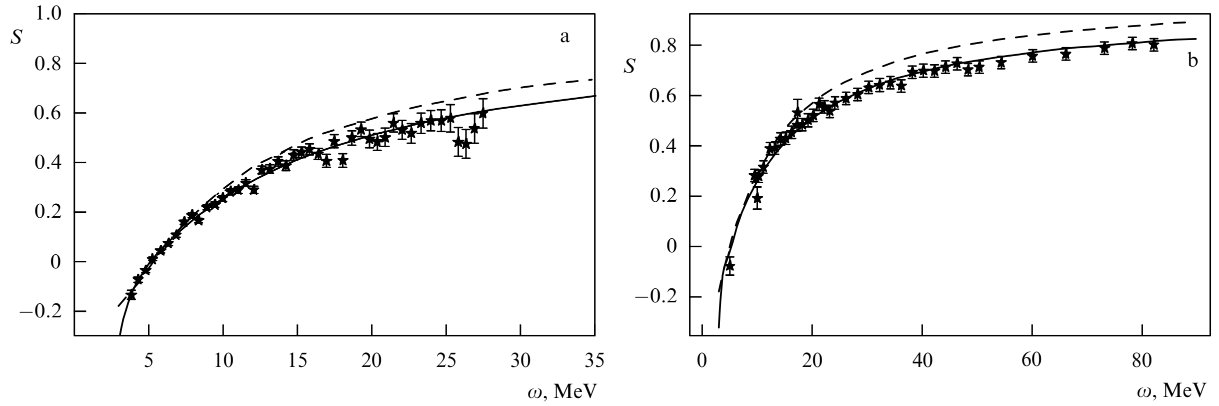

Figure 8. Dependence of $S = (\sigma_{\rm coh} - \sigma_{\rm B})/\sigma_{\rm C}^{(0)}$ on ω: (a) $Z = 83$ (bismuth), and (b) $Z = 82$ (lead). Solid curve — results of work [31], and dashed curve — results of work [30]. Experimental data are borrowed from Ref. [39] for bismuth, and from Refs [40, 41] for lead.

The cross section $\mathrm{d}\sigma_{\rm B}/\mathrm{d}\mathbf{q}$ vanishes as $\beta_p \to 0$, but the cross section exact in η is not zero in this limit:

$$\frac{\mathrm{d}\sigma}{\mathrm{d}\mathbf{q}} = \frac{4\alpha}{\omega\Delta^4}\exp(-\pi\eta)\sum_{l=1}^{\infty} l^3 (2\eta)^{2\gamma+1}\,\frac{|\Gamma(\gamma - \mathrm{i}\eta)|^2}{\Gamma^2(2\gamma+1)} \times \left(|\mathcal{G}_1|^2 + 2\eta^2|\mathcal{G}_2|^2 - 2\eta\,\mathrm{Im}\,(\mathcal{G}_1^*\mathcal{G}_2)\right), \tag{40}$$

$$\mathcal{G}_1 = F(\gamma - \mathrm{i}\eta,\, 2\gamma+1,\, 2\mathrm{i}\eta)\,, \quad \mathcal{G}_2 = \frac{F(\gamma+1-\mathrm{i}\eta,\, 2\gamma+2,\, 2\mathrm{i}\eta)}{2\gamma+1}\,,$$

where $\gamma = \sqrt{l^2 - \eta^2}$. For $\eta \ll 1$, formula (40) has the asymptotics

$$\frac{\mathrm{d}\sigma}{\mathrm{d}\mathbf{q}} = \frac{8\alpha\eta^3}{\omega\Delta^4}\,. \tag{41}$$

The ratio of cross section $\mathrm{d}\sigma/\mathrm{d}\mathbf{q}$ (40) and asymptotics (41) depending on η is plotted in Fig. 9. It can be seen that higher-order terms in η substantially change the result obtained in the approximation lowest in η. Note that cross section $\mathrm{d}\sigma/\mathrm{d}\mathbf{p}$ disappears in the $\beta_q \to 0$ limit, because the wave function for slow positrons is exponentially suppressed at distances on the order of $\lambda_{\rm C} = 1/m$.

As $\beta_p \to 1$, the difference $\mathrm{d}\sigma/\mathrm{d}\mathbf{q} - \mathrm{d}\sigma_{\rm B}/\mathrm{d}\mathbf{q}$ (Coulomb corrections) tends toward zero, as is seen in Fig. 10 wherein this difference is presented in units of $S_1 = \alpha\eta^2/(\omega\Delta^4)$ as a function of β_p. An analogous assertion is true of the difference $\mathrm{d}\sigma/\mathrm{d}\mathbf{p} - \mathrm{d}\sigma_{\rm B}/\mathrm{d}\mathbf{p}$ as $\beta_q = q/\varepsilon_q \to 1$. This fact can be explained as follows. The main contribution to Coulomb corrections is determined by impact parameters ρ on the order of $\lambda_{\rm C}$, but in the kinematics being discussed one has $\rho \ll \lambda_{\rm C}$ as $\beta_{p,q} \to 1$.

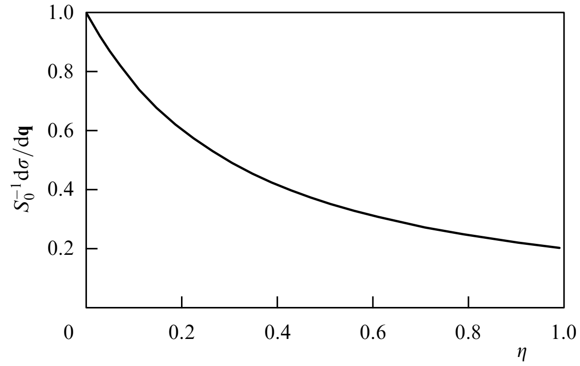

Figure 9. Dependence of $\mathrm{d}\sigma/\mathrm{d}\mathbf{q}$ (in units of $S_0 = 8\alpha\eta^3/\omega\Delta^4$) on η as $\beta_p \to 0$.

In Fig. 11, cross section $\mathrm{d}\sigma/\mathrm{d}\mathbf{q}$ in units of S_1 is plotted as a function of β_p throughout the entire interval of its allowed values and for several Z values. It illustrates the importance of Coulomb corrections for all β_p with the exception of region near point $\beta_p = 1$.

The authors of Ref. [32] studied the spectrum of electrons in energy regions $\varepsilon_p \sim m$ and $\varepsilon_q \sim m$. The Z-dependence of $\omega\,\mathrm{d}\sigma/\mathrm{d}\varepsilon_p$ (in units of $\tilde{\sigma} = \alpha\eta^3/m^2$) at a zero electron velocity is shown in Fig. 12 by the solid curve. As $\eta \to 0$, we have the asymptotics $\omega\,\mathrm{d}\sigma/\mathrm{d}\varepsilon_p = 4\pi\tilde{\sigma}$. Reference [43] proposes a

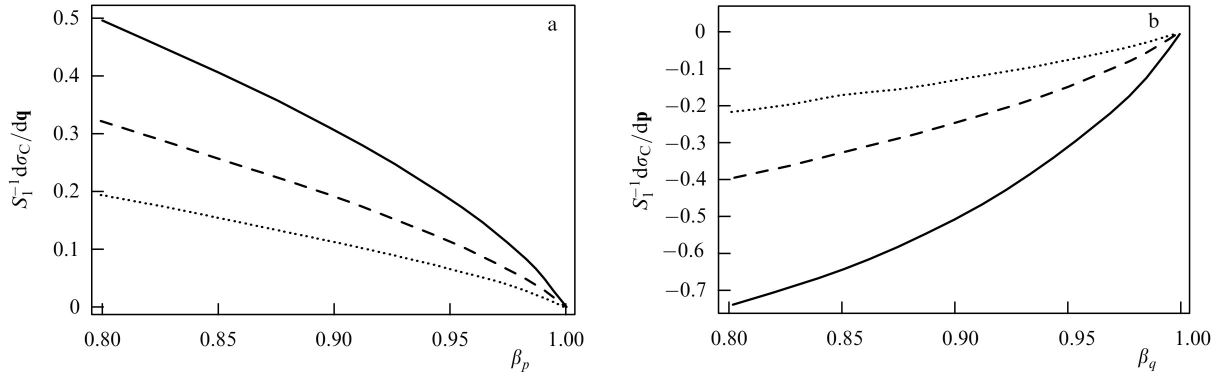

Figure 10. Variations of (a) $\mathrm{d}\sigma_{\rm C}/\mathrm{d}\mathbf{q} = \mathrm{d}\sigma/\mathrm{d}\mathbf{q} - \mathrm{d}\sigma_{\rm B}/\mathrm{d}\mathbf{q}$ in units of $S_1 = \alpha\eta^2/(\omega\Delta^4)$ as a function of β_p near $\beta_p = 1$, and (b) $\mathrm{d}\sigma_{\rm C}/\mathrm{d}\mathbf{p} = \mathrm{d}\sigma/\mathrm{d}\mathbf{p} - \mathrm{d}\sigma_{\rm B}/\mathrm{d}\mathbf{p}$ in S_1 units as a function of β_q near $\beta_q = 1$. Solid curve — $Z = 92$, dashed curve — $Z = 47$, and dotted curve — $Z = 26$.

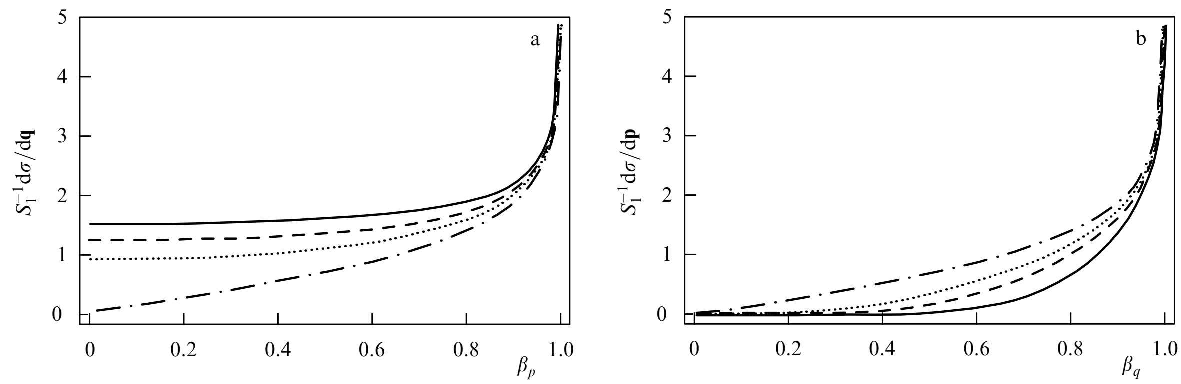

Figure 11. (a) Cross section $\mathrm{d}\sigma/\mathrm{d}\mathbf{q}$ in units of $S_1 = \alpha\eta^2/(\omega\Delta^4)$ as a function of β_p. (b) Cross section $\mathrm{d}\sigma/\mathrm{d}\mathbf{p}$ in units of S_1 as a function of β_q. Solid curve — $Z = 92$, dashed curve — $Z = 47$, dotted curve — $Z = 26$, and dash-dotted curve — $Z = 1$.

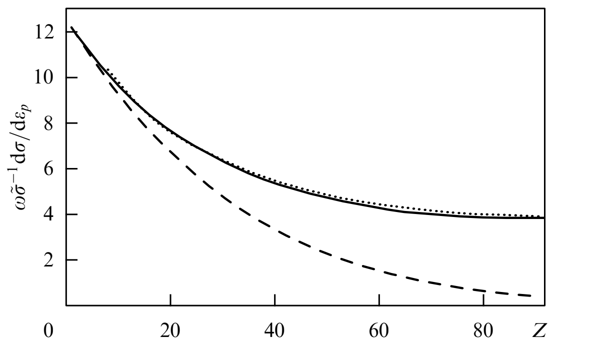

Figure 12. Cross section $\omega\tilde{\sigma}^{-1}\,\mathrm{d}\sigma/\mathrm{d}\varepsilon_p$ at zero electron velocity in units of $\tilde{\sigma} = \alpha\eta^3/m^2$: results of Refs [32] (solid curve), [43] (dashed curve) [see Eqn (42)], and [6] (dotted curve) obtained from exact formulas at $\omega = 40$ MeV and $\beta_p = 0.1265$.

formula for $\omega\,\mathrm{d}\sigma/\mathrm{d}\varepsilon_p$ at zero electron velocity:

$$\omega\,\frac{\mathrm{d}\sigma}{\mathrm{d}\varepsilon_p} = 4\pi\,\frac{\alpha\eta^3}{m^2}\,\frac{2\pi\eta}{\exp(2\pi\eta) - 1}\left(1 - \frac{4\pi}{15}\,\eta\right). \tag{42}$$

The result of tabulation of this formula is presented in Fig. 12 by the dotted curve. It is evidenced that formula (42) is applicable only at small η values. Notice that cross section $\omega\,\mathrm{d}\sigma_{\mathrm{B}}/\mathrm{d}\varepsilon_p$ in the Born approximation tends to zero in the $\beta_p \to 0$ limit, because the cross section $\omega\,\mathrm{d}\sigma_{\mathrm{B}}/\mathrm{d}\varepsilon_p \approx 2\alpha\eta^2\beta_p/m^2$ for $\beta_p \ll 1$. In Ref. [6], the cross section $\omega\,\mathrm{d}\sigma/\mathrm{d}\varepsilon$ was found with the use of exact formulas [5] at $\omega = 40$ MeV and $\varepsilon_p = 1.008\,m$ (corresponding to $\beta_p = 0.1265$). This result is drawn in Fig. 12 by the dotted curve starting from $Z = 11$. There is excellent agreement between the results of Refs [6] and [32]. They differ at $Z = 1$, because the Born term contribution becomes important at small Z and $\beta_p = 0.1265$.

The Born cross section $\mathrm{d}\sigma_{\mathrm{B}}/\mathrm{d}\varepsilon$ for $\omega \gg m$ and $p \ll \omega$ is well known [4]:

$$\frac{\mathrm{d}\sigma_{\mathrm{B}}}{\mathrm{d}\varepsilon_p} = \frac{\sigma_0}{\omega}\,\frac{2\varepsilon_p}{p^3}\left[2\varepsilon_p\,p\ln\left(\frac{\varepsilon_p + p}{m}\right) - p^2 - m^2\ln^2\left(\frac{\varepsilon_p + p}{m}\right)\right]. \tag{43}$$

Specifically, $\mathrm{d}\sigma_{\mathrm{B}}/\mathrm{d}\varepsilon_p = 2\sigma_0\,p/m$ for $p \ll m$, and for $p \gg m$ one has

$$\frac{\mathrm{d}\sigma_{\mathrm{B}}}{\mathrm{d}\varepsilon_p} = \frac{4\sigma_0}{\omega}\left[\ln\left(\frac{2\varepsilon_p}{m}\right) - \frac{1}{2}\right]. \tag{44}$$

The Coulomb correction to $\mathrm{d}\sigma/\mathrm{d}\varepsilon_p$ was deduced in the leading quasiclassical approximation for $\omega \gg p \gg m$ in Ref. [8]:

$$\frac{\mathrm{d}\sigma_{\mathrm{C}}^{(0)}}{\mathrm{d}\varepsilon_p} = -\frac{4\sigma_0}{\omega}\,f(\eta)\,, \tag{45}$$

where function $f(\eta)$ was defined in Eqn (15). Correction (45) is independent of ε_p; it remains the same for an electron and a positron, thus being an even function of η. The first-order quasiclassical correction to relation (45) was found in paper [31]:

$$\frac{\mathrm{d}\sigma_{\mathrm{C}}^{(1)}}{\mathrm{d}\varepsilon_p} = \frac{\sigma_0}{\omega}\,\frac{\pi^3 m}{2\varepsilon_p}\,\mathrm{Re}\,g(\eta)\,, \tag{46}$$

where function $g(\eta)$ was given in Eqn (15). Formulas (44)–(46) correspond to the asymptotics of formulas (26) at small $x = \varepsilon_p/\omega$.

Correction (46) has the opposite sign for an electron and a positron, since $g(\eta)$ (the odd function of η) increases the cross section for slow electrons, and decreases it for slow positrons. Results from Ref. [32] for Coulomb corrections $\omega\sigma_0^{-1}\,\mathrm{d}\sigma_{\mathrm{C}}/\mathrm{d}\varepsilon_{p,q} = \omega\sigma_0^{-1}(\mathrm{d}\sigma/\mathrm{d}\varepsilon_{p,q} - \mathrm{d}\sigma_{\mathrm{B}}/\mathrm{d}\varepsilon_{p,q})$ to the spectra of slow electrons and slow positrons are depicted in Figs 13 and 14 by solid curves for several Z values. They are compared with asymptotic expressions $\omega\sigma_0^{-1}\,\mathrm{d}\sigma_{\mathrm{C}}^{(0)}/\mathrm{d}\varepsilon_{p,q}$ (dashed curve) and $\omega\sigma_0^{-1}(\mathrm{d}\sigma_{\mathrm{C}}^{(0)}/\mathrm{d}\varepsilon_{p,q} + \mathrm{d}\sigma_{\mathrm{C}}^{(1)}/\mathrm{d}\varepsilon_{p,q})$ (dotted curve). Clearly, the result of paper [32] for each Z value tends, at high energies, toward a constant value of $-4f(\eta)$. On the other hand, consideration of the correction $\mathrm{d}\sigma_{\mathrm{C}}^{(1)}/\mathrm{d}\varepsilon_{p,q}$ considerably improves the agreement between exact and asymptotic results for slow electrons and positrons.

Correction $\sigma_{\mathrm{C}}^{(1)}$ can be derived based on the results of Ref. [32] from the formula

$$\sigma_{\mathrm{C}}^{(1)} = \int_m^\infty \mathrm{d}\varepsilon_p\left(\frac{\mathrm{d}\sigma_{\mathrm{C}}}{\mathrm{d}\varepsilon_p} + \frac{\mathrm{d}\sigma_{\mathrm{C}}}{\mathrm{d}\varepsilon_p}(\eta \to -\eta) + \frac{8\sigma_0 f(\eta)}{\omega}\right). \tag{47}$$

Numerical integration of formula (4) is consistent with Eqn (35).

4. Single bremsstrahlung of relativistic particles in an atomic field

The bremsstrahlung cross section in the Born approximation is known for any particle energy and arbitrary atomic form factor [2, 3] (see also monograph [4]). The bremsstrahlung

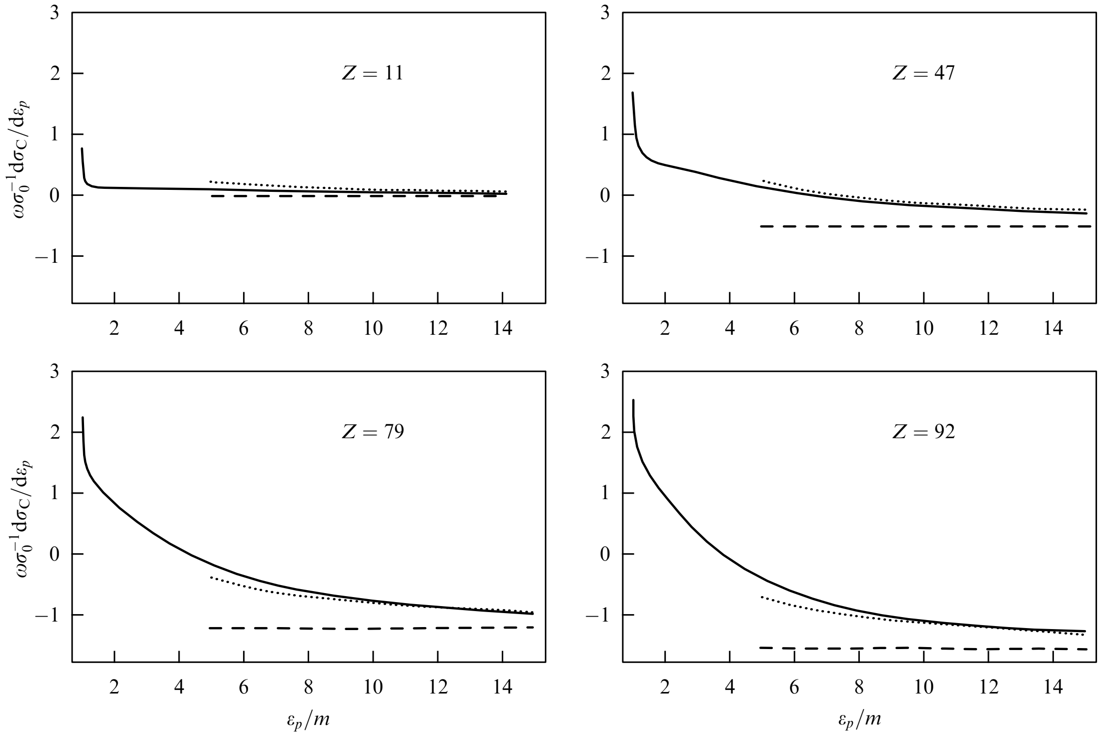

Figure 13. Dependence of Coulomb corrections $\omega\sigma_0^{-1}\,\mathrm{d}\sigma_\mathrm{C}/\mathrm{d}\varepsilon_p$ in units of $\sigma_0 = \alpha\eta^2/m^2$ on electron energy ε_p in units of m (solid curve) for several Z values. The dashed curve corresponds to the Coulomb leading correction in the $\varepsilon_p \gg m$ limit, and the dotted curve includes corrections proportional to m/ε_p.

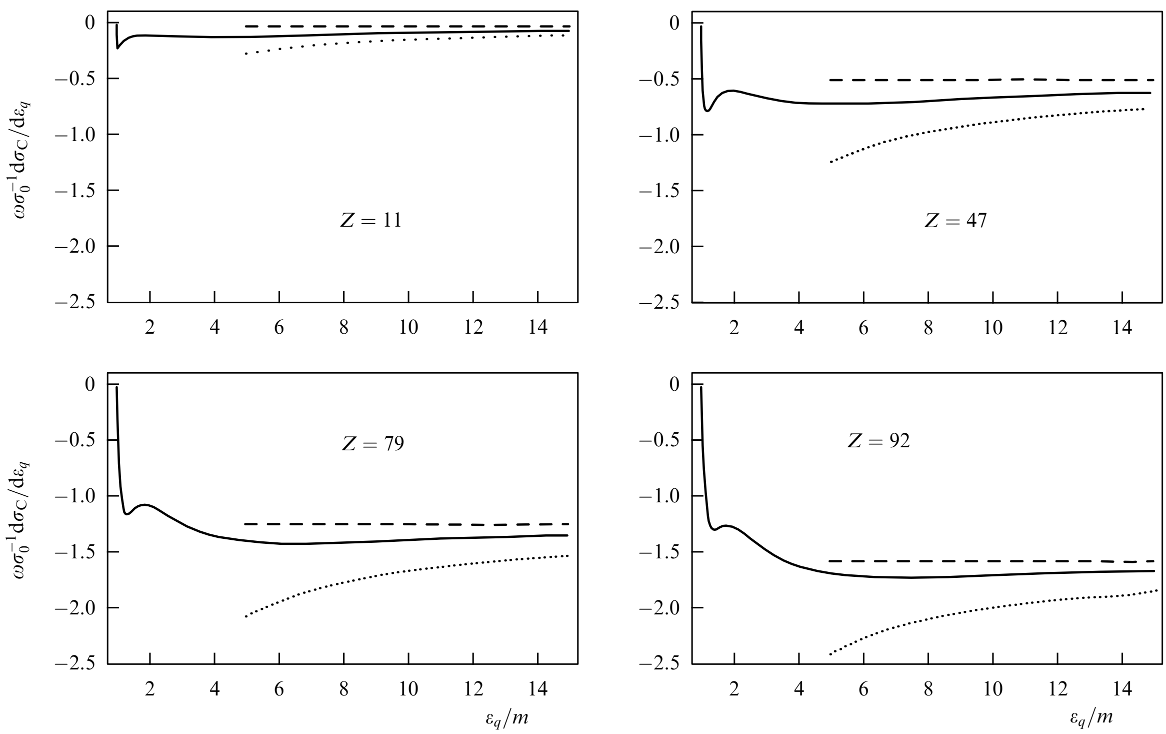

Figure 14. Dependence of Coulomb corrections $\omega\sigma_0^{-1}\,\mathrm{d}\sigma_\mathrm{C}/\mathrm{d}\varepsilon_q$ in units of $\sigma_0 = \alpha\eta^2/m^2$ on positron energy ε_q in units of m (solid curve) for several Z values. The dashed curve represents the Coulomb leading correction in the $\varepsilon_q \gg m$ limit, and the dotted curve includes corrections proportional to m/ε_q. Dashed and dotted curves begin from $\varepsilon_q = 5\,m$, since they correspond to asymptotics found for $\varepsilon_q \gg m$.

cross section was deduced in the leading quasiclassical approximation in Refs [7–9, 44, 45]. The first-order quasi-classical correction to the bremsstrahlung spectrum was calculated in Refs [31, 46]. As was mentioned in the foregoing, the influence of a field screening on Coulomb corrections to the photoproduction cross section is insignificant. The influence of screening on bremsstrahlung in the atomic field, unlike its effect on photoproduction, is highly nontrivial. It was shown in papers [9, 46] that Coulomb corrections to the bremsstrahlung differential cross section are very sensitive to screening. However, Coulomb corrections to the cross section integrated over momenta of the final charged particle are independent of screening in the leading approximation in parameter $1/mr_{\rm scr} \ll 1$, where $r_{\rm scr} \sim Z^{-1/3}(m\alpha)^{-1}$ is the screening radius. A quantitative evaluation of the screening effect on Coulomb corrections to the bremsstrahlung spectrum was undertaken in Ref. [46]. The bremsstrahlung differential cross section calculated in the leading quasiclassical approximation proved identical for electrons and positrons (for μ^+ and μ^-). This means that the first-order quasiclassical correction needs to be taken into consideration in order to predict the charge asymmetry (the difference between bremsstrahlung differential cross sections of a particle and antiparticle in the atomic field), as was done in Ref. [20]. The result thus obtained is exact in the parameter η. For muons, the finite nucleus size effect was additionally taken into account.

4.1 Bremsstrahlung differential cross section

Let us consider the bremsstrahlung differential cross section for a relativistic charged particle with momentum $\mathbf{p}$ and helicity $\mu_p = \pm 1$ in the atomic potential $V(\mathbf{r})$, which is summarized over the photon helicity and helicity of the final charged particle with momentum $\mathbf{q}$.

Given that the first-order quasiclassical correction is taken into consideration, this cross section has the form [20]

$$\begin{aligned}
&\mathrm{d}\sigma(\mathbf{p},\mathbf{q},\mathbf{k},\eta) = \frac{2\alpha\varepsilon_q^2}{\omega m^2 (2\pi)^4}\,\mathrm{d}\Omega_{\mathbf{k}}\,\mathrm{d}\Omega_{\mathbf{q}}\,\mathrm{d}\omega\,(S_0+S_1+S_2)\,,\\
&S_0 = |A_0|^2\left[\frac{\Delta^2}{m^2}(\varepsilon_p^2+\varepsilon_q^2)\xi_p\xi_q - 2\varepsilon_p\varepsilon_q(\xi_p-\xi_q)^2\right],\\
&S_1 = \mathrm{Re}\,A_0A_1^*\left\{\frac{\Delta^2}{m^2}(\varepsilon_p^2+\varepsilon_q^2)(\varepsilon_p+\varepsilon_q)\xi_p\xi_q\right.\\
&\qquad\left.+\left[(\varepsilon_p^2+\varepsilon_q^2)(\varepsilon_p-\varepsilon_q) - 4\varepsilon_p\varepsilon_q(\varepsilon_p\xi_p-\varepsilon_q\xi_q)\right](\xi_p-\xi_q)\right\},\\
&S_2 = -\frac{2\mu_p}{m^2}\,\mathrm{Im}\,A_0A_1^*\,\omega^2(\varepsilon_p+\varepsilon_q)\xi_p\xi_q\,[\mathbf{p}_\perp\times\mathbf{q}_\perp]\,\mathbf{v}\,,
\end{aligned}\tag{48}$$

where $\mathrm{d}\Omega_{\mathbf{k}}$ and $\mathrm{d}\Omega_{\mathbf{q}}$ are the solid angles corresponding to photon momentum $\mathbf{k}$ and momentum $\mathbf{q}$, respectively, while $\omega = \varepsilon_p - \varepsilon_q$ is photon energy. It is assumed that $\varepsilon_p \gg m$ and $\varepsilon_q \gg m$. The following notations were introduced into Eqn (48):

$$\begin{aligned}
&A_0 = -\frac{\mathrm{i}}{\Delta_\perp^2}\int\mathrm{d}\mathbf{r}\,\exp\left(-\mathrm{i}\boldsymbol{\Delta}\mathbf{r} - \mathrm{i}\chi(\rho)\right)\boldsymbol{\Delta}_\perp\boldsymbol{\nabla}_\perp V(\mathbf{r})\,,\\
&A_1 = -\frac{1}{2\varepsilon_p\varepsilon_q}\int\mathrm{d}\mathbf{r}\,\exp\left(-\mathrm{i}\boldsymbol{\Delta}\mathbf{r} - \mathrm{i}\chi(\rho)\right)\\
&\qquad\times\int_0^\infty \mathrm{d}x\,x\,\boldsymbol{\nabla}_\perp V(\mathbf{r}-x\mathbf{v})\boldsymbol{\nabla}_\perp V(\mathbf{r})\,,\\
&\chi(\rho) = \int_{-\infty}^{\infty} V(z,\boldsymbol{\rho})\,\mathrm{d}z\,,\quad \xi_p = \frac{m^2}{m^2+p_\perp^2}\,,\quad \xi_q = \frac{m^2}{m^2+q_\perp^2}\,;
\end{aligned}\tag{49}$$

the z-axis is directed along the unit vector $\mathbf{v} = \mathbf{k}/\omega$; $\boldsymbol{\Delta} = \mathbf{q}+\mathbf{k}-\mathbf{p}$ stands for momentum transfer, and $\boldsymbol{\Delta}_\perp$, $\boldsymbol{\rho}$, $\mathbf{p}_\perp$, and $\mathbf{q}_\perp$ are components of vectors $\boldsymbol{\Delta}$, $\mathbf{r}$, $\mathbf{p}$, and $\mathbf{q}$ perpendicular to vector $\mathbf{v}$.

Cross section $\mathrm{d}\sigma(\mathbf{p},\mathbf{q},\mathbf{k},\eta)$ can be represented as the sum

$$\begin{aligned}
&\mathrm{d}\sigma(\mathbf{p},\mathbf{q},\mathbf{k},\eta) = \mathrm{d}\sigma_{\rm s}(\mathbf{p},\mathbf{q},\mathbf{k},\eta) + \mathrm{d}\sigma_{\rm a}(\mathbf{p},\mathbf{q},\mathbf{k},\eta)\,,\\
&\mathrm{d}\sigma_{\rm s}(\mathbf{p},\mathbf{q},\mathbf{k},\eta) = \frac{\mathrm{d}\sigma(\mathbf{p},\mathbf{q},\mathbf{k},\eta) + \mathrm{d}\sigma(\mathbf{p},\mathbf{q},\mathbf{k},-\eta)}{2}\,,\\
&\mathrm{d}\sigma_{\rm a}(\mathbf{p},\mathbf{q},\mathbf{k},\eta) = \frac{\mathrm{d}\sigma(\mathbf{p},\mathbf{q},\mathbf{k},\eta) - \mathrm{d}\sigma(\mathbf{p},\mathbf{q},\mathbf{k},-\eta)}{2}\,.
\end{aligned}\tag{50}$$

Evidently, the bremsstrahlung differential cross section of an antiparticle can be derived from $\mathrm{d}\sigma(\mathbf{p},\mathbf{q},\mathbf{k},\eta)$ by the substitution $\eta \to -\eta$, so that it will equal $\mathrm{d}\sigma_{\rm s}(\mathbf{p},\mathbf{q},\mathbf{k},\eta) - \mathrm{d}\sigma_{\rm a}(\mathbf{p},\mathbf{q},\mathbf{k},\eta)$. In the leading quasiclassical approximation, the entire η dependence of the cross section is associated with factor $|A_0|^2$ in term S_0 from (48). Because $A_0 \to -A_0^*$ at $\eta \to -\eta$, cross sections calculated in the leading quasiclassical approximation are identical for particles and antiparticles. Item S_1 is the odd function of η determining the antisymmetric part of cross section $\mathrm{d}\sigma_{\rm a}(\mathbf{p},\mathbf{q},\mathbf{k},\eta)$. Item S_2 is the even function of η that contributes to the symmetric part of cross section $\mathrm{d}\sigma_{\rm s}(\mathbf{p},\mathbf{q},\mathbf{k},\eta)$ and disappears after averaging over helicity μ_p of the initial particle. To recall, term S_2 is responsible for cross section asymmetry with respect to substitution $\varphi_i \to -\varphi_i$, where φ_i are azimuthal emission angles of final particles in a system with the z-axis directed along vector $\mathbf{p}$. Such asymmetry is absent in the cross section calculated in the leading quasiclassical approximation. It should be noted that terms S_1 and S_2 differ from zero only if the next-to-leading-order (quasiclassical) contribution is taken into consideration. Importantly, the antisymmetric part of cross section, $\mathrm{d}\sigma_{\rm a}(\mathbf{p},\mathbf{q},\mathbf{k},\eta)$, is independent of screening in the kinematics region making the main contribution to the antisymmetric part of the cross section.

Coefficients A_0 and A_1 depend on $\mathbf{p}$, $\mathbf{q}$, and $\mathbf{k}$ momenta only through the dependence on momentum transfer $\boldsymbol{\Delta}$. It is therefore easy to write down the formula for the cross section $\mathrm{d}\sigma/\mathrm{d}\omega\,\mathrm{d}\boldsymbol{\Delta}_\perp$:

$$\begin{aligned}
&\frac{\mathrm{d}\sigma_{\rm s}}{\mathrm{d}\omega\,\mathrm{d}\boldsymbol{\Delta}_\perp} = \frac{\alpha\varepsilon_q}{2\pi^3\omega\varepsilon_p}|A_0|^2\Phi(\zeta)\,,\\
&\frac{\mathrm{d}\sigma_{\rm a}}{\mathrm{d}\omega\,\mathrm{d}\boldsymbol{\Delta}_\perp} = \frac{\alpha\varepsilon_q(\varepsilon_p+\varepsilon_q)}{2\pi^3\omega\varepsilon_p}\,\mathrm{Re}\,A_0A_1^*\Phi\,,\\
&\Phi = \frac{\ln\left(\zeta+\sqrt{1+\zeta^2}\right)}{\zeta\sqrt{1+\zeta^2}}\left(\zeta^2\,\frac{\varepsilon_p^2+\varepsilon_q^2}{\varepsilon_p\varepsilon_q}+1\right) - 1\,,\quad \zeta = \frac{\Delta_\perp}{2m}\,.
\end{aligned}\tag{51}$$

4.2 Coulomb corrections to electron bremsstrahlung cross section

The main contribution to Coulomb corrections to the symmetrical part of the bremsstrahlung differential cross section comes from the $\Delta \sim \max(r_{\rm scr}^{-1}, \Delta_{\min})$ region [9, 46], where $\Delta_{\min} = p - q - \omega \approx m^2\omega/(2\varepsilon_q\varepsilon_p)$. Indeed, screening can be neglected in the $\Delta \gg \max(r_{\rm scr}^{-1}, \Delta_{\min})$ region, $V(r)$ substituted by the Coulomb potential $V_{\rm C}(r) = -\eta/r$, and component $\Delta_\parallel$ disregarded in view of its smallness compared with $\Delta_\perp$. Then, a simple calculation leads to the following formulas for the coefficients in contributions S_0, S_1, and S_2 in Eqn (48):

$$|A_0|^2 = \left(\frac{4\pi\eta}{\Delta^2}\right)^2,\quad \left\{\begin{matrix}\mathrm{Re}\,A_0A_1^*\\ \mathrm{Im}\,A_0A_1^*\end{matrix}\right\} = \frac{\pi\Delta}{4\varepsilon_p\varepsilon_q}|A_0|^2\left\{\begin{matrix}\mathrm{Re}\,g(\eta)\\ \mathrm{Im}\,g(\eta)\end{matrix}\right\},\tag{52}$$

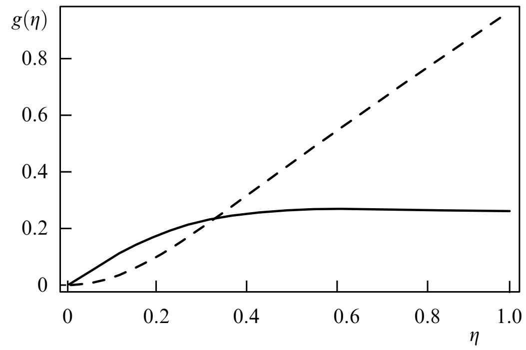

Figure 15. Graphs of functions $\mathrm{Re}\,g(\eta)$ (solid curve) and $-\mathrm{Im}\,g(\eta)$ (dashed curve).

where $g(\eta)$ was defined in Eqn (15). Thus, $|A_0|^2$ coincides with its Born $|A_{0\mathrm{B}}|^2$ value. The η dependences of terms S_1 in $\mathrm{d}\sigma_\mathrm{a}$ and S_2 in $\mathrm{d}\sigma_\mathrm{s}$ are determined by functions $\mathrm{Re}\,g(\eta)$ and $\mathrm{Im}\,g(\eta)$ shown in Fig. 15. For $\eta \ll 1$, one has $\mathrm{Re}\,g(\eta) \approx \eta$ and $\mathrm{Im}\,g(\eta) \approx -(4\ln 2)\eta^2$. It follows from Fig. 15 that $\mathrm{Re}\,g(\eta)$ and $\mathrm{Im}\,g(\eta)$ are significantly different from their asymptotic values even at very small η.

For $\omega \ll \varepsilon_p$, the ratio of asymmetric-to-symmetric parts of the cross section is given by

$$\frac{S_1}{S_0} = \frac{\pi\Delta\,\mathrm{Re}\,g(\eta)}{2\varepsilon_p}\,, \tag{53}$$

it increases with Δ/ε_p and can exceed 10%. The S_2/S_0 ratio is small for $\omega \ll \varepsilon_p$, when it is suppressed by factor $(\omega/\varepsilon_p)^2$.

If $|\mathbf{p}_\perp| \gg m$ and $|\mathbf{q}_\perp| \gg m$, then

$$\frac{S_1}{S_0} = \frac{\pi\,\mathrm{Re}\,g(\eta)}{2\Delta}\,\boldsymbol{\Delta}\,\boldsymbol{\theta}_{qp}\,, \quad \frac{S_2}{S_0} = \mu_p\,\frac{\pi\omega(\varepsilon_p+\varepsilon_q)\,\mathrm{Im}\,g(\eta)}{2(\varepsilon_p^2+\varepsilon_q^2)\Delta}\,[\boldsymbol{\Delta}\times\boldsymbol{\theta}_{qp}]\mathbf{v}\,, \tag{54}$$

where $\boldsymbol{\theta}_{qp} = \mathbf{p}_\perp/p - \mathbf{q}_\perp/q$, meaning that azimuthal asymmetry enhances with ω and may acquire importance.

Let us discuss the cross section $\mathrm{d}\sigma/\mathrm{d}\omega\,\mathrm{d}\boldsymbol{\Delta}_\perp$ in the case of $\Delta \gg \max(r_\mathrm{scr}^{-1}, \Delta_\mathrm{min})$ [see Eqn (51)]:

$$\begin{aligned} \frac{\mathrm{d}\sigma_\mathrm{s}}{\mathrm{d}\omega\,\mathrm{d}\boldsymbol{\Delta}_\perp} &= \frac{8\alpha\eta^2\varepsilon_q}{\pi\omega\varepsilon_p\Delta_\perp^4}\,\Phi\,, \\ \frac{\mathrm{d}\sigma_\mathrm{a}}{\mathrm{d}\omega\,\mathrm{d}\boldsymbol{\Delta}_\perp} &= \frac{\pi\,\mathrm{Re}\,g(\eta)(\varepsilon_p+\varepsilon_q)\Delta}{4\varepsilon_p\varepsilon_q}\,\frac{\mathrm{d}\sigma_\mathrm{s}}{\mathrm{d}\omega\,\mathrm{d}\boldsymbol{\Delta}_\perp}\,, \end{aligned} \tag{55}$$

where function Φ is defined in Eqn (51). Figure 16 illustrates the dependence of $A = \sigma_{0\mathrm{a}}^{-1}\,\mathrm{d}\sigma_\mathrm{a}/\mathrm{d}\omega\,\mathrm{d}\boldsymbol{\Delta}_\perp$ on $\zeta = \Delta_\perp/(2m)$ for several values of $t = \varepsilon_q/\varepsilon_p$, with $\sigma_{0\mathrm{a}} = \alpha\eta^2\,\mathrm{Re}\,g(\eta)/(2m^2\omega\varepsilon_p\Delta_\perp)$. It is readily seen that the main contribution to the antisymmetric part of the cross section is determined by the $\Delta \sim m$ region.

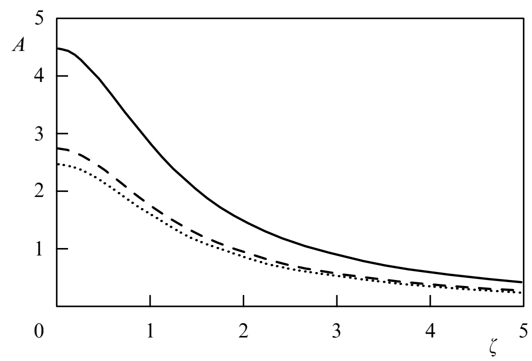

Figure 16. Dependence of $A = \sigma_{0\mathrm{a}}^{-1}\,\mathrm{d}\sigma_\mathrm{a}/\mathrm{d}\omega\,\mathrm{d}\boldsymbol{\Delta}_\perp$ on $\zeta = \Delta_\perp/(2m)$ [Eqn (55)], with $\sigma_{0\mathrm{a}} = \alpha\eta^2\,\mathrm{Re}\,g(\eta)/(2m^2\omega\varepsilon_p\Delta_\perp)$ at $t = \varepsilon_q/\varepsilon_p$: $t = 0.25$ (solid curve), $t = 0.5$ (dashed curve), and $t = 0.75$ (dotted curve).

It is somewhat more difficult to obtain the cross section integrated over final electron angles. Substituting expressions (52) for $|A_0|^2$, $\mathrm{Re}\,A_0A_1^*$, and $\mathrm{Im}\,A_0A_1^*$ into Eqn (48) and integrating over $\mathbf{q}$ yield

$$\begin{aligned} \frac{\mathrm{d}\sigma_\mathrm{s}}{\mathrm{d}\mathbf{k}} &= \frac{4\alpha\eta^2\xi_p^2}{\pi m^4\omega^3}\left\{(\varepsilon_p^2+\varepsilon_q^2)L - \varepsilon_p\varepsilon_q\left[1 + 4\xi_p(1-\xi_p)\left(L - \frac{3}{2}\right)\right]\right\}, \\ \frac{\mathrm{d}\sigma_\mathrm{a}}{\mathrm{d}\mathbf{k}} &= \frac{\pi\alpha\eta^2\,\mathrm{Re}\,g(\eta)}{m^3\omega^3\varepsilon_p\varepsilon_q}\,\xi_p \\ &\quad\times\left[\varepsilon_q(\varepsilon_p^2+\varepsilon_q^2+2\varepsilon_p\omega\xi_p)F_1 + \xi_p(\varepsilon_p^2\omega - \varepsilon_q^3 - 4\varepsilon_p\varepsilon_q\omega\xi_p)F_2\right], \\ L &= \ln\left(\frac{2\varepsilon_p\varepsilon_q}{m\omega}\right) - \frac{1}{2} - f(\eta)\,, \\ F_1 &= F\left(\frac{1}{2}, \frac{1}{2}; 1; -\frac{p_\perp^2}{m^2}\right) = \frac{2}{\pi}\,K\left(-\frac{p_\perp^2}{m^2}\right), \\ F_2 &= F\left(-\frac{1}{2}, \frac{1}{2}; 1; -\frac{p_\perp^2}{m^2}\right) = \frac{2}{\pi}\,E\left(-\frac{p_\perp^2}{m^2}\right), \end{aligned} \tag{56}$$

where $K(x)$ and $E(x)$ are the elliptic functions.

The antisymmetric part of the spectrum is found by integrating cross section (51) over $\boldsymbol{\Delta}_\perp$ [31, 46]:

$$\frac{\mathrm{d}\sigma_\mathrm{a}}{\mathrm{d}\omega} = \frac{\alpha\pi^3\eta^2\,\mathrm{Re}\,g(\eta)}{4m\omega\varepsilon_p^2}\left(2\,\frac{\varepsilon_p^2+\varepsilon_q^2}{\varepsilon_p\varepsilon_q} - 1\right)(\varepsilon_p+\varepsilon_q)\,. \tag{57}$$

To determine the Coulomb correction to the symmetric part of the bremsstrahlung spectrum, it is necessary to consider the $\Delta \sim \max(r_\mathrm{scr}^{-1}, \Delta_\mathrm{min})$ region. It was revealed in Ref. [46] that quantity $|A_0(\Delta)|^2$ in this region greatly depends on screening. However, Coulomb corrections to the symmetric part of the spectrum are a universal function of η and independent of screening because [46]

$$\int \Delta_\perp^2\left[|A_0(\Delta)|^2 - |A_{0\mathrm{B}}(\Delta)|^2\right]\mathrm{d}\boldsymbol{\Delta}_\perp = -32\pi^3\eta^2 f(\eta)\,. \tag{58}$$

As a result [9], one arrives at

$$\frac{\mathrm{d}\sigma_\mathrm{C}}{\mathrm{d}\omega} = -\frac{4\alpha\eta^2 f(\eta)}{m^2\omega}\left(\frac{\varepsilon_q^2}{\varepsilon_p^2} - \frac{2\varepsilon_q}{3\varepsilon_p} + 1\right). \tag{59}$$

Thus, $\mathrm{d}\sigma/\mathrm{d}\omega$ in the Coulomb field takes the form

$$\frac{\mathrm{d}\sigma}{\mathrm{d}\omega} = \frac{4\alpha\eta^2}{m^2\omega}\left(\frac{\varepsilon_q^2}{\varepsilon_p^2} - \frac{2\varepsilon_q}{3\varepsilon_p} + 1\right)L\,, \tag{60}$$

where function L was defined in Eqn (56). The result of accounting for screening in the Born contribution to the spectrum is well known [12] and not discussed in this review.

4.3 Coulomb corrections to muon bremsstrahlung cross section

Studies of Coulomb corrections to the bremsstrahlung differential cross section for relativistic muons in an atomic field must take into consideration the effect of the finite nuclear size R (the difference between $V(r)$ and Coulomb potentials at distances $r \lesssim R$). This issue was addressed in paper [20], taking into consideration the first-order quasi-classical correction. Let us write out Fourier transform

$V_F(\Delta^2)$ of the $V(r)$ potential in the form

$$V_F(\Delta^2) = -\frac{4\pi\eta F(\Delta^2)}{\Delta^2}\,, \tag{61}$$

where $F(\Delta^2)$ is the form factor significantly different from unity for $\Delta \gtrsim 1/R$ and $\Delta \lesssim 1/r_{\rm scr}$. Let us first consider the Coulomb corrections to the symmetrical part of the cross section calculated in the leading quasiclassical approximation. In this case, the cross section $d\sigma_s$ depends on field parameters only through factor A_0 (49). In the Born approximation, one finds

$$A_{0\rm B} = -\frac{\rm i}{\Delta_\perp^2}\int {\rm d}\mathbf{r}\,\exp\left(-{\rm i}\boldsymbol{\Delta}\mathbf{r}\right)\boldsymbol{\Delta}_\perp\boldsymbol{\nabla}_\perp V(\mathbf{r}) = V_F(\Delta^2)\,. \tag{62}$$

Coulomb corrections $|A_0|^2 - |A_{0\rm B}|^2$ disappear for $r_{\rm scr}^{-1} \ll \Delta \ll R^{-1}$ and have two peaks at $\Delta \sim r_{\rm scr}^{-1}$ and $\Delta \sim R^{-1}$. Contributions from these peaks to integral $\int \Delta_\perp^2 \left[|A_0|^2 - |A_{0\rm B}|^2\right] {\rm d}\boldsymbol{\Delta}_\perp$ are opposite in sign and equal $\mp 32\pi^3\eta^2 f(\eta)$, respectively. Both are universal functions of η independent of the shape of the potential in the $r \sim r_{\rm scr}$ and $r \sim R$ regions, whereas the peak shape is highly sensitive there to the type of potential [9, 46]. Because the condition $m \ll R^{-1}$ is satisfied for electrons, the contribution to Coulomb corrections to $d\sigma_s/d\omega$ comes only from the $r \sim r_{\rm scr}$ region [9]. For muons, however, the contributions of both peaks have to be summarized on the assumption that the condition $m_\mu \gg R^{-1}$ is fulfilled. As a result, the total Coulomb correction disappears in the cross section integrated over $\Delta_\perp$. It should be emphasized once again that Coulomb corrections to the differential cross section at $\Delta \sim R^{-1}$ and $\Delta \sim r_{\rm scr}^{-1}$ are rather large. To illustrate this fact, we shall consider the form factor $F(\Delta^2)$ as given by formula (21) that holds for $\Delta \gg r_{\rm scr}^{-1}$ transfers for which A_0 is defined by the formula

$$\begin{aligned} A_0 &= -\frac{4\pi\eta}{\Delta^2}\int_0^\infty {\rm d}\rho\, J_1(\rho)\left[1 - \frac{\Lambda\rho}{\Delta}\,K_1\!\left(\frac{\Lambda\rho}{\Delta}\right)\right] \\ &\quad\times \exp\left\{-2{\rm i}\eta\left[\ln\frac{\rho}{2} + K_0\!\left(\frac{\Lambda\rho}{\Delta}\right)\right]\right\}, \\ A_{0\rm B} &= -\frac{4\pi\eta}{\Delta^2 + \Lambda^2}\,. \end{aligned} \tag{63}$$

Here, $J_n(x)$ is the Bessel function, and $K_n(x)$ is the modified Bessel function of the second kind. Figure 17 demonstrates the dependence of the relative value of Coulomb corrections, $|A_0|^2/|A_{0\rm B}|^2 - 1$, on Δ/Λ at several η values. The very narrow peak at $\Delta \sim r_{\rm scr}^{-1}$ is not shown in the figure. A detailed study on the dependence of this peak on the shape of the atomic potential at $\Delta \sim r_{\rm scr}^{-1}$ is reported in Ref. [46]. It follows from Fig. 17 that Coulomb corrections to $|A_0|^2$ are very large in the $\Delta/\Lambda \sim 1$ region.

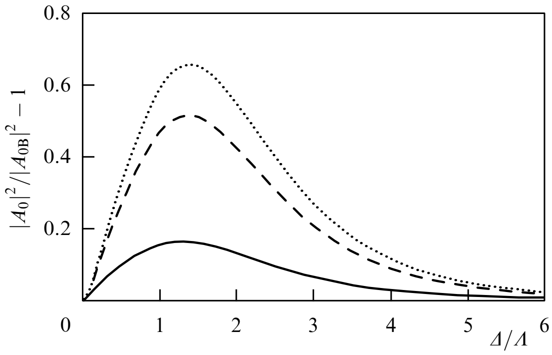

Figure 17. Relative value of Coulomb corrections as a function of Δ/Λ for $\Delta \gg 1/r_{\rm scr}$ and $\eta = 0.34$ (silver, solid curve), $\eta = 0.6$ (lead, dashed curve), and $\eta = 0.67$ (uranium, dotted curve).

Let us next consider the quantity A_1 [see formula (49)]. Its lowest-order approximation in η, $A_{1\rm B}$, is expressed through the same integral $J(\Delta)$ (19) that was included in the correction to $\mu^+\mu^-$-pair photoproduction cross section:

$$A_{1\rm B}(\Delta) = -\frac{J(\Delta)}{2\varepsilon_p\varepsilon_q}\,. \tag{64}$$

Factor A_1 exact in η can be represented for $\Delta \gg r_{\rm scr}^{-1}$ as

$$\begin{aligned} A_1(\Delta) &= \int_0^\infty\!\!\int_0^\infty {\rm d}x\,{\rm d}\rho\, A_{1\rm B}\!\left(\frac{\Delta x}{\rho\Lambda}\right) J_0(\rho) J_0(x) \\ &\quad\times \exp\left\{-2{\rm i}\eta\left[\ln\frac{\rho}{2} + K_0\!\left(\frac{\rho\Lambda}{\Delta}\right)\right]\right\}. \end{aligned} \tag{65}$$

For the nuclear form factor (21), $A_{1\rm B}(\Delta)$ is expressed through the function $\mathcal{F}$ defined in Eqn (22):

$$A_{1\rm B}(\Delta) = -\frac{\pi^2\eta^2\Lambda^2\mathcal{F}}{\varepsilon_p\varepsilon_q\Delta(\Lambda^2 + \Delta^2)}\,. \tag{66}$$

Figure 18 demonstrates the dependences of G_1 and G_2 on the $\beta = \Delta/\Lambda$ ratio:

$$\begin{aligned} G_1 &= \frac{{\rm Re}\,A_0A_1^*}{|A_0|^2\Sigma_{\rm R}}\,, \quad \Sigma_{\rm R} = \frac{\pi\,{\rm Re}\,g(\eta)\Delta}{4\varepsilon_p\varepsilon_q}\,, \\ G_2 &= \frac{{\rm Im}\,A_0A_1^*}{|A_0|^2\Sigma_{\rm I}}\,, \quad \Sigma_{\rm I} = \frac{\pi\,{\rm Im}\,g(\eta)\Delta}{4\varepsilon_p\varepsilon_q}\,. \end{aligned} \tag{67}$$

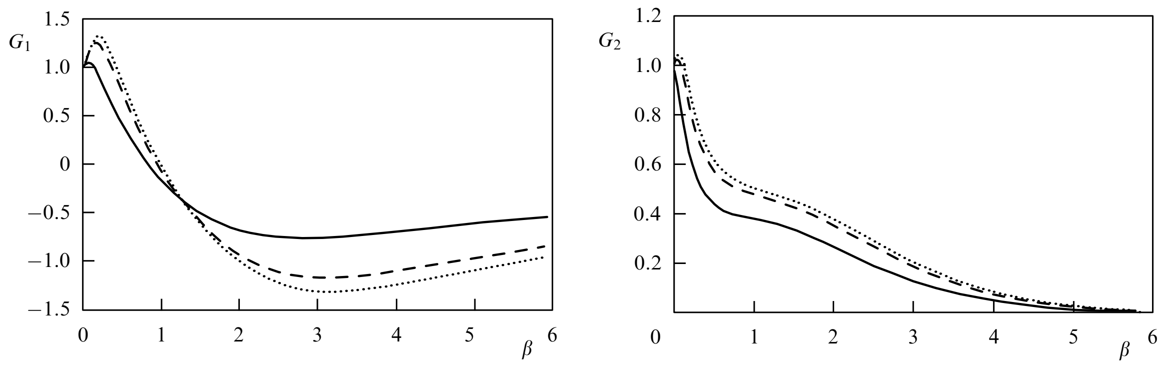

Figure 18. Dependences of $G_1 = \Sigma_{\rm R}^{-1}\,{\rm Re}\,A_0A_1^*/|A_0|^2$ and $G_2 = \Sigma_{\rm I}^{-1}\,{\rm Im}\,A_0A_1^*/|A_0|^2$ on $\beta = \Delta/\Lambda$ [see Eqn (67)] at $\eta = 0.34$ (silver, solid curve), $\eta = 0.6$ (lead, dashed curve), and $\eta = 0.67$ (uranium, dotted curve).

In the Coulomb field, $G_1 = G_2 = 1$ [see Eqn (52)]. Therefore, the difference of $G_{1,2}$ from unity is due to the finite nucleus size effect. Evidently, G_1 and G_2 rapidly decrease with increasing β for $\beta \lesssim 1$.

5. Double bremsstrahlung of a relativistic charged particle in an atomic field

The double bremsstrahlung of an electron in an atomic field had until recently been investigated either at low electron energies [47, 48] or at any electron energies in the Born approximation [49]. A recent study [50] in the leading quasiclassical approximation yielded the double bremsstrahlung differential cross section, exact in η, for a relativistic electron in an atomic field. It turned out that Coulomb corrections to the double bremsstrahlung differential cross section are very sensitive to a field screening effect.

Moreover, these Coulomb corrections are present in the same factor A_0 (49) as in the case of the single bremsstrahlung differential cross section calculated in the leading quasiclassical approximation [46]. As a result, the cross section $d\sigma$ of double bremsstrahlung can be represented as the sum of the Born contribution $d\sigma^{\rm B}$ and Coulomb corrections $d\sigma^{\rm C}$:

$$d\sigma_{\mu_p\mu_q\lambda_1\lambda_2} = d\sigma^{\rm B}_{\mu_p\mu_q\lambda_1\lambda_2} + d\sigma^{\rm C}_{\mu_p\mu_q\lambda_1\lambda_2}\,,$$

$$\begin{Bmatrix} d\sigma^{\rm B}_{\mu_p\mu_q\lambda_1\lambda_2} \\ d\sigma^{\rm C}_{\mu_p\mu_q\lambda_1\lambda_2}\end{Bmatrix} = \frac{\alpha^2}{(2\pi)^6\omega_1\omega_2}\, d\mathbf{k}_1\, d\mathbf{k}_2\, d\mathbf{\Delta}_\perp \times \begin{Bmatrix} \left|A_{0\rm B}(\mathbf{\Delta})\right|^2 \\ \left[\left|A_0(\mathbf{\Delta})\right|^2 - \left|A_{0\rm B}(\mathbf{\Delta})\right|^2\right]\end{Bmatrix} \left|\mathcal{T}_{\mu_p\mu_q\lambda_1\lambda_2}\right|^2\,, \qquad (68)$$

$$\mathcal{T}_{\mu_p\mu_q\lambda_1\lambda_2} = \mathbf{\Delta}_\perp\left[\mathbf{T}_{\mu_p\mu_q\lambda_1\lambda_2}(\mathbf{k}_1,\mathbf{k}_2,\mathbf{\Delta}_\perp) + \mathbf{T}_{\mu_p\mu_q\lambda_2\lambda_1}(\mathbf{k}_2,\mathbf{k}_1,\mathbf{\Delta}_\perp)\right]\,,$$

where $\mathbf{k}_{1,2}$, $\omega_{1,2}$ are momenta and energies of final photons, $\mathbf{\Delta} = \mathbf{q}+\mathbf{k}_1+\mathbf{k}_2-\mathbf{p}$, $\mathbf{p}$ and $\mathbf{q}$ are initial and final momenta of a charged particle, $\mathbf{\Delta}_\perp$ is the component $\mathbf{\Delta}$ perpendicular to vector $\mathbf{p}$, μ_p, μ_q, λ_1, λ_2 are helicities of the initial and final electrons and emitted photons, and $\mathbf{T}_{\mu_p\mu_q\lambda_1\lambda_2}(\mathbf{k}_1,\mathbf{k}_2,\mathbf{\Delta}_\perp)$ is the η-independent quantity whose explicit form was presented in paper [50]. Similar to the case of single bremsstrahlung, only the region of small $\Delta_\perp \sim \max(r_{\rm scr}^{-1}, |\Delta_\parallel|) \ll m$ contributes to $d\sigma^{\rm C}$. As mentioned above, despite the high sensitivity of $|A_0(\mathbf{\Delta})|^2 - |A_{0\rm B}(\mathbf{\Delta})|^2$ to screening, Coulomb corrections to the cross section integrated over $\mathbf{\Delta}_\perp$ are insensitive to the shape of the atomic potential at $r \sim r_{\rm scr}$ [46]:

$$d\sigma^{\rm C}_{\mu_p\mu_q\lambda_1\lambda_2} = -\frac{\alpha^2\eta^2 f(\eta)}{4\pi^3\omega_1\omega_2}\, d\mathbf{k}_1\, d\mathbf{k}_2 \times \left|\mathbf{T}^{(0)}_{\mu_p\mu_q\lambda_1\lambda_2}(\mathbf{k}_1,\mathbf{k}_2) + \mathbf{T}^{(0)}_{\mu_p\mu_q\lambda_2\lambda_1}(\mathbf{k}_2,\mathbf{k}_1)\right|^2\,, \qquad (69)$$

where $\mathbf{T}^{(0)}_{\mu_p\mu_q\lambda_1\lambda_2}(\mathbf{k}_1,\mathbf{k}_2) = \mathbf{T}_{\mu_p\mu_q\lambda_1\lambda_2}(\mathbf{k}_1,\mathbf{k}_2,0)$. The main contribution to the Born cross section integrated over $d\mathbf{\Delta}_\perp$ is determined by the region of small $\Delta_\perp$, i.e., $m \gg \Delta_\perp \gg m\beta$, with

$$\beta = \max\left\{\frac{1}{mr_{\rm scr}}\,, \frac{|\Delta_\parallel|}{m}\right\}\,,$$
$$\Delta_\parallel = -\frac{1}{2}\left[\frac{q_\perp^2}{q} + \frac{k_{1\perp}^2}{\omega_1} + \frac{k_{2\perp}^2}{\omega_2} + \frac{m^2(\omega_1+\omega_2)}{pq}\right]\,, \qquad (70)$$

where $\mathbf{q}_\perp$, $\mathbf{k}_{1\perp}$, and $\mathbf{k}_{2\perp}$ are components of vectors $\mathbf{q}$, $\mathbf{k}_1$, and $\mathbf{k}_2$ normal to vector $\mathbf{p}$. As $\ln(1/\beta) \gg 1$, we have within logarithmic accuracy the following relation

$$d\sigma^{\rm B}_{\mu_p\mu_q\lambda_1\lambda_2} = \frac{\alpha^2\eta^2}{4\pi^3\omega_1\omega_2}\, d\mathbf{k}_1\, d\mathbf{k}_2 \ln\frac{1}{\beta} \times \left|\mathbf{T}^{(0)}_{\mu_p\mu_q\lambda_1\lambda_2}(\mathbf{k}_1,\mathbf{k}_2) + \mathbf{T}^{(0)}_{\mu_p\mu_q\lambda_2\lambda_1}(\mathbf{k}_2,\mathbf{k}_1)\right|^2\,. \qquad (71)$$

To demonstrate the angular dependence of Coulomb corrections, let us introduce a dimensionless quantity S defined as

$$S = \frac{m^6}{2}\sum_{\mu_p\mu_q\lambda_1\lambda_2}\left|\mathbf{T}^{(0)}_{\mu_p\mu_q\lambda_1\lambda_2}(\mathbf{k}_1,\mathbf{k}_2) + \mathbf{T}^{(0)}_{\mu_p\mu_q\lambda_2\lambda_1}(\mathbf{k}_2,\mathbf{k}_1)\right|^2\,. \qquad (72)$$

Figure 19a illustrates the dependence of S on $\delta_2 = pk_{2\perp}/(m\omega_2)$ at fixed values of $\delta_1 = pk_{1\perp}/(m\omega_1)$, ω_1/ε_p, ω_2/ε_p, and the azimuthal angle φ between vectors $\mathbf{k}_{1\perp}$ and $\mathbf{k}_{2\perp}$. Figure 19b plots the dependence of S on φ at fixed values of δ_1, δ_2, ω_1/ε_p, and ω_2/ε_p. Notice that S is invariant with respect to the substitution $\varphi \to -\varphi$. It follows from Fig. 19 that S exhibits a smooth angular dependence.

Figure 20 presents the δ_1-dependence of S at fixed values of ω_1/ε_p and ω_2/ε_p, where

$$S_1 = \frac{p^2}{16\pi^2 m^2}\int S\, d\Omega_{\mathbf{k}_2}\,, \qquad (73)$$

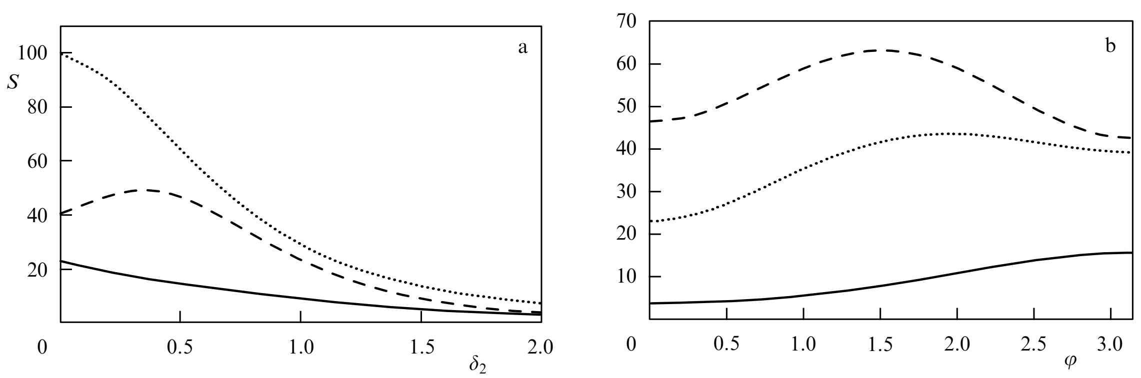

Figure 19. (a) Dependence of S (72) on $\delta_2 = pk_{2\perp}/(m\omega_2)$ at $\omega_1/\varepsilon_p = 0.2$, $\omega_2/\varepsilon_p = 0.4$, $\varphi = 0$, $\delta_1 = pk_{1\perp}/(m\omega_1) = 0.2$ (dashed curve), $\delta_1 = 1$ (dotted curve), and $\delta_1 = 2$ (solid curve). (b) The dependence of S (72) on azimuthal angle φ between vectors $\mathbf{k}_{1\perp}$ and $\mathbf{k}_{2\perp}$ at $\omega_1/\varepsilon_p = 0.2$, $\omega_2/\varepsilon_p = 0.4$, $\delta_1 = 0.2$, $\delta_2 = 0.5$ (dashed curve), $\delta_2 = 1$ (dotted curved), and $\delta_2 = 2$ (solid curve).

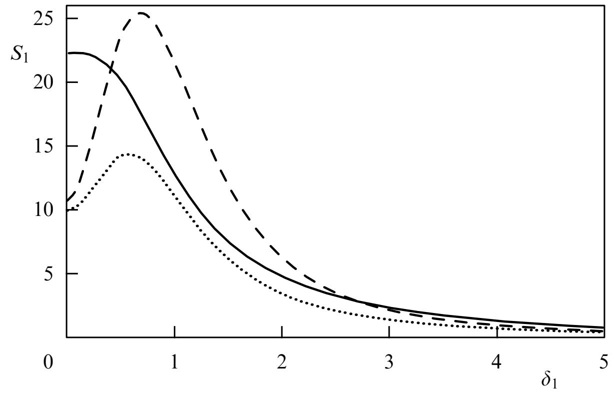

Figure 20. Dependence of S_1 (73) on δ_1 at $\omega_1/\varepsilon_p = \Omega x$ and $\omega_2/\varepsilon_p = \Omega(1-x)$, where $\Omega = 0.4$, $x = 0.3$ (dashed curve), $x = 0.5$ (dotted curve), and $x = 0.7$ (solid curve).

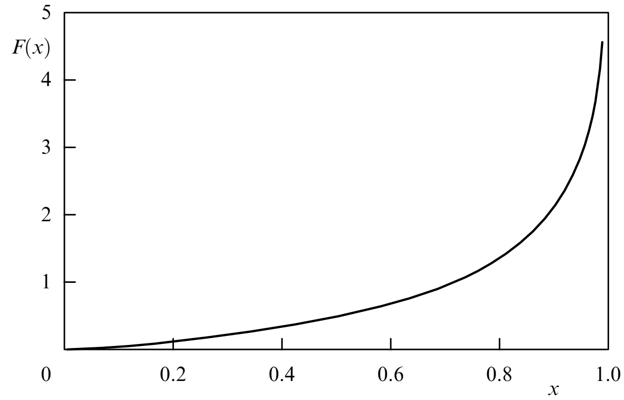

Figure 21. Dependence of $F(x)$ on $x = \omega_1/\varepsilon_p$ [Eqn (75)].

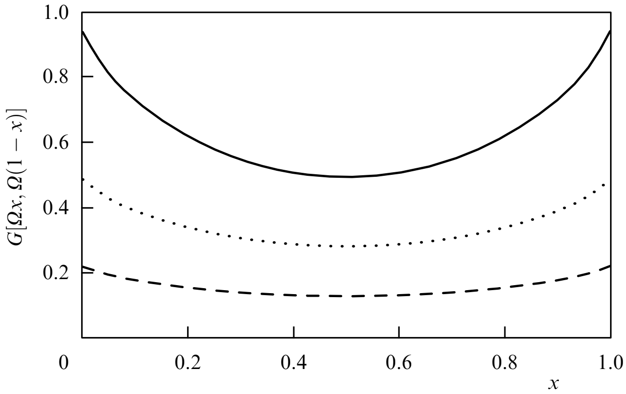

Figure 22. Dependence of $G[\Omega x, \Omega(1-x)]$ on x (74) at $\Omega = 0.3$ (dashed curve), $\Omega = 0.5$ (dotted curve), and $\Omega = 0.7$ (solid curve). Here, $\Omega = (\omega_1+\omega_2)/\varepsilon_p$, and $x = \omega_1/(\omega_1+\omega_2)$.

suggesting that the main contribution to the cross section is determined by the $\delta_1 \sim 1$ region.

Let us consider now the Coulomb corrections to the cross section integrated over $d\Omega_{\mathbf{k}_1}$ and $d\Omega_{\mathbf{k}_2}$ (Coulomb corrections to the spectrum) averaged over polarization of the initial electron and summarized over final particle polarizations:

$$d\sigma^{\mathrm{C}} = -\frac{8\alpha^2\eta^2 f(\eta)\, d\omega_1\, d\omega_2}{\pi m^2\omega_1\omega_2}\, G\left(\frac{\omega_1}{\varepsilon_p}, \frac{\omega_2}{\varepsilon_p}\right), \tag{74}$$

where function $f(\eta)$ was defined in Eqn (15), and the function $G(\omega_1/\varepsilon_p, \omega_2/\varepsilon_p)$ for arbitrary frequencies is found by numerical integration of the cross section (69) over photon emission angles. The result for $\omega_2 \ll \omega_1, \varepsilon_q$ corresponds to the soft photon approximation [4]:

$$F(x) = G(x,0) = \int_0^\infty \frac{dy}{(1+y)^2}\left[1+(1-x)^2 - \frac{4y(1-x)}{(1+y)^2}\right]\Phi(x,y)\,,$$
$$\Phi(x,y) = \frac{t}{\sqrt{t^2-1}}\ln\left(t+\sqrt{t^2-1}\right) - 1\,, \quad t = 1 + \frac{x^2(1+y)}{2(1-x)}\,. \tag{75}$$

Function $F(x)$ is shown in Fig. 21. It possesses the following asymptotics:

$$F(x) \approx \frac{4}{3}x^2 \ln\frac{1}{x} \quad \text{for} \quad x \ll 1\,,$$
$$F(x) \approx \ln\frac{1}{1-x} \quad \text{for} \quad 1-x \ll 1\,. \tag{76}$$

Figure 22 demonstrates the dependence of the function $G[\Omega x, \Omega(1-x)]$ on x at fixed Ω values, where $\Omega = (\omega_1+\omega_2)/\varepsilon_p$, and $x = \omega_1/(\omega_1+\omega_2)$.

In the Born approximation, the spectrum has, within a logarithmic accuracy, the shape

$$d\sigma^{\mathrm{B}} = \frac{8\alpha^2\eta^2\, d\omega_1\, d\omega_2}{\pi m^2\omega_1\omega_2}\, G\left(\frac{\omega_1}{\varepsilon_p}, \frac{\omega_2}{\varepsilon_p}\right)\ln\frac{1}{\beta_0}\,, \tag{77}$$

where function G is the same as in Eqn (74), and

$$\beta_0 = \max\left\{\frac{1}{mr_{\mathrm{scr}}}, \frac{m(\omega_1+\omega_2)}{\varepsilon_p\varepsilon_q}\right\} \ll 1\,. \tag{78}$$

To conclude, study [50] on the double bremsstrahlung differential cross section, exact in η, for a relativistic particle in an atomic field showed that in the leading quasiclassical approximation the potential enters the process cross section only through the factor $|A_0(\mathbf{\Delta})|^2$. This factor coincides with the analogous factor in the single bremsstrahlung cross section calculated in the leading quasiclassical approximation. It should be emphasized that such factorization is violated by taking account of the first-order quasiclassical correction [20]. Study [50] made it possible to formulate a simple method for calculating exactly in η the multiple bremsstrahlung cross section in the leading quasiclassical approximation. To this end, it is necessary to find the cross section in the Born approximation for an arbitrary potential $V(r)$ and then substitute the factor $A_0(\mathbf{\Delta})$ from Eqn (49) for the Fourier transform $V_F(\Delta^2)$ of the potential.

6. Photoproduction of an e^+e^- pair accompanied by photon emission

Photoproduction of an e^+e^- pair in an atomic field accompanied by photon emission ($\gamma Z \to e^+e^-\gamma' Z$) makes an important contribution to radiation corrections to an e^+e^--pair photoproduction and serves as a background for Delbrück scattering [21]. The $\gamma Z \to e^+e^-\gamma' Z$ process also needs to be taken into account in the investigation of electromagnetic showers in matter. Despite the obvious importance of this process, there are only a few publications in which it has been considered in the Born approximation

[51, 52], while the results, exact in parameter η, are altogether absent due to the computational difficulties. In recent work [53], the differential cross section of the $\gamma Z \to e^+e^-\gamma' Z$ process was calculated, exactly in η, in the leading quasiclassical approximation.

It turned out that Coulomb corrections change the result considerably in comparison with the Born approximation except in a narrow region of very small momentum transfers.

The cross section of the process has the form

$$d\sigma_{\lambda_1\lambda_2\mu_p\mu_q} = \alpha^2|M_{\lambda_1\lambda_2\mu_p\mu_q}|^2 \frac{d\mathbf{p}_\perp\, d\mathbf{q}_\perp\, d\mathbf{k}_{2\perp}\, d\varepsilon_p\, d\varepsilon_q}{(2\pi)^6\omega_1\omega_2}, \quad (79)$$

where $\mathbf{k}_1$, $\mathbf{k}_2$, $\mathbf{p}$, and $\mathbf{q}$ are the momenta of the initial photon, final photon, electron, and positron, respectively; λ_1, λ_2, μ_p, and μ_q are the helicities of the initial photon, final photon, electron, and positron, and $\mathbf{X}_\perp$ denotes the component of vector $\mathbf{X}$ normal to the $\mathbf{k}_1$ vector directed along the z-axis. Amplitude M may be represented as the sum $M = M^{\rm B} + M^{\rm C}$, where $M^{\rm B}$ is the term linear in η (Born amplitude), and $M^{\rm C}$ is the contribution from higher-order terms in η (Coulomb corrections). Representation of the Born amplitude found in Ref. [53] has the form

$$M^{\rm B}_{\lambda_1\lambda_2\mu_p\mu_q} = \frac{64\pi\eta}{\omega_1\omega_2\Delta^2}\left[\mathcal{F}_{\lambda_1\lambda_2\mu_p\mu_q}(\boldsymbol{\Delta}_\perp) - \mathcal{F}_{\lambda_1\lambda_2\mu_p\mu_q}(-\boldsymbol{\Delta}_\perp)\right], \quad (80)$$

where $\boldsymbol{\Delta} = \mathbf{p} + \mathbf{q} + \mathbf{k}_2 - \mathbf{k}_1$ is the momentum transfer, and $\mathcal{F}_{\lambda_1\lambda_2\mu_p\mu_q}(\mathbf{T})$ are certain elementary functions, the explicit form of which was reported in paper [53]. The Coulomb corrections are also expressed through these functions:

$$\begin{aligned} M^{\rm C}_{\lambda_1\lambda_2\mu_p\mu_q} = &-\frac{128 i\eta^2}{\omega_1\omega_2\Delta^2}\int \frac{d\mathbf{T}}{(\mathbf{T}+\boldsymbol{\Delta}_\perp)^2(\mathbf{T}-\boldsymbol{\Delta}_\perp)^2}\left(\frac{|\mathbf{T}+\boldsymbol{\Delta}_\perp|}{|\mathbf{T}-\boldsymbol{\Delta}_\perp|}\right)^{2i\eta} \\ &\times\Big\{(\boldsymbol{\Delta}_\perp^2 + \mathbf{T}\boldsymbol{\Delta}_\perp)\left[\mathcal{F}_{\lambda_1\lambda_2\mu_p\mu_q}(\mathbf{T}) - \mathcal{F}_{\lambda_1\lambda_2\mu_p\mu_q}(\boldsymbol{\Delta}_\perp)\right] \\ &+ (\boldsymbol{\Delta}_\perp^2 - \mathbf{T}\boldsymbol{\Delta}_\perp)\left[\mathcal{F}_{\lambda_1\lambda_2\mu_p\mu_q}(\mathbf{T}) - \mathcal{F}_{\lambda_1\lambda_2\mu_p\mu_q}(-\boldsymbol{\Delta}_\perp)\right]\Big\}, \end{aligned} \quad (81)$$

where $\mathbf{T}$ is the two-dimensional vector normal to $\mathbf{k}_1$. The screening effect is important only for the small momentum transfer $\Delta \lesssim r_{\rm scr}^{-1} \ll m$, where $r_{\rm scr}$ is the screening radius. For such Δ, Coulomb corrections can be neglected. Therefore, the screening effect can be taken into account via multiplying $M^{\rm B}_{\lambda_1\lambda_2\mu_p\mu_q}$ by an atomic form factor $F_{\rm a}(\Delta^2)$, which is equal to unity for $\Delta \gg r_{\rm scr}^{-1}$.

Figure 23 depicts the dependence of S (differential cross section in units of γ averaged over initial photon polarization and summarized over final particle polarizations):

$$S = \frac{1}{2}\sum_{\lambda_1\lambda_2\mu_p\mu_q} \frac{\gamma^{-1}\, d\sigma_{\lambda_1\lambda_2\mu_p\mu_q}}{d\mathbf{p}_\perp\, d\mathbf{q}_\perp\, d\mathbf{k}_{2\perp}\, d\varepsilon_p\, d\varepsilon_q}, \quad \gamma = \frac{\alpha^2\eta^2\Delta_\perp^2}{(2\pi)^6 m^6\omega_1\omega_2\Delta^4}, \quad (82)$$

on k_{2x} at fixed values of $\mathbf{p}_\perp$, $\mathbf{q}_\perp$, ε_p, ε_q, $k_{2y} = 0$, and several values of the atomic charge number Z. In the vicinity of point $\Delta_\perp = 0$ ($k_{2x} = -3.9m$), the Born cross section dominates over Coulomb corrections, as it must. In general, however, Coulomb corrections considerably change the Born result. To recall, the value of S in the Coulomb field is independent of ω_1 at fixed ε_p/ω_1, ε_q/ω_1, $\mathbf{p}_\perp/m$, $\mathbf{q}_\perp/m$, and $\mathbf{k}_{2\perp}/m$ values. For an atomic field, S depends on ω_1 only due to the atomic form factor. But this form factor is essential only in the vicinity of point $\Delta_\perp = 0$, where Coulomb corrections are of no consequence.

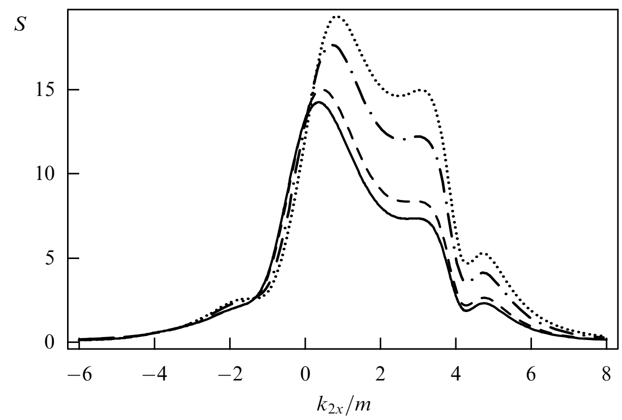

Figure 23. Dependence of S (differential cross section in units of γ averaged over initial photon polarization and summarized over final particle polarizations (82) on k_{2x}/m for $\varepsilon_p = 0.4\omega_1$, $\varepsilon_q = 0.25\omega_1$, $p_x = 4.7m$, $q_x = -0.8m$, and $p_y = q_y = k_{2y} = 0$: the Born result (dotted curve), $Z = 47$ (silver, dash-dotted curve), $Z = 82$ (lead, dashed curve), and $Z = 92$ (uranium, solid curve). S calculated for the Coulomb field is unrelated to ω_1. Account of screening where ω_1-dependence through the form factor is preserved changes S only in a small vicinity of point $\Delta_\perp = 0$ ($k_{2x} = -3.9\,m$ in the figure), where Coulomb corrections are of no consequence.

Then there appears an interesting problem of A asymmetry of the differential cross section for circular polarization of the initial photon:

$$A = \frac{d\sigma_+ - d\sigma_-}{d\sigma_+ + d\sigma_-}, \qquad d\sigma_\pm = \sum_{\lambda_2\mu_p\mu_q} d\sigma_{\pm\lambda_2\mu_p\mu_q}. \quad (83)$$

In the Born approximation, asymmetry is absent for any $\mathbf{p}$, $\mathbf{q}$, or $\mathbf{k}_2$. This fact ensues from the relation

$$M^{\rm B}_{\lambda_1\lambda_2\mu_p\mu_q} = -\mu_p\mu_q\left(M^{\rm B}_{\bar\lambda_1\bar\lambda_2\bar\mu_p\bar\mu_q}\right)^*. \quad (84)$$

However, this relation is invalid for Coulomb corrections due to the presence of complex factor $(|\mathbf{T}+\boldsymbol{\Delta}_\perp|/|\mathbf{T}-\boldsymbol{\Delta}_\perp|)^{2i\eta}$ in the integrand of the expression in Eqn (81). Figure 24 plots the dependence of asymmetry on the φ angle between vectors

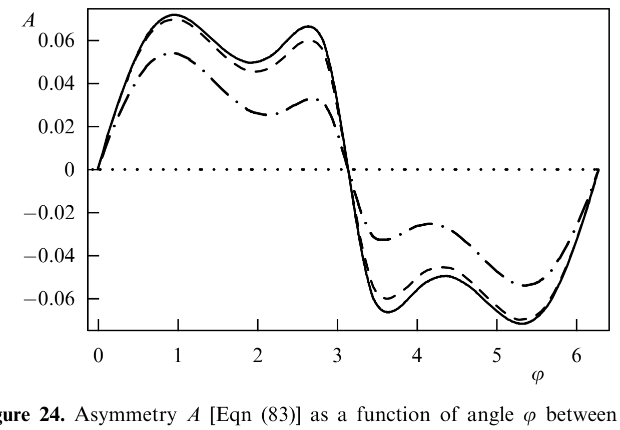

Figure 24. Asymmetry A [Eqn (83)] as a function of angle φ between vectors $\mathbf{k}_{2\perp}$ and $\mathbf{p}_\perp$ for $\varepsilon_p = 0.4\omega_1$, $\varepsilon_q = 0.25\omega_1$, $\mathbf{p}_\perp \| -\mathbf{q}_\perp$, $p_\perp = 4.7m$, $q_\perp = 0.8m$, and $k_{2\perp} = m$: the Born result — dotted curve, $Z = 47$ (silver) — dash-dotted curve, $Z = 82$ (lead) — dashed curve, and $Z = 92$ (uranium) — solid curve.

$\mathbf{k}_{2\perp}$ and $\mathbf{p}_\perp$. As it must, the asymmetry disappears for $\mathbf{k}_1, \mathbf{k}_2, \mathbf{p}$, and $\mathbf{q}$ lying in one plane ($\varphi = 0, \pi$). Clearly, asymmetry can be as large as a few dozen percent even at moderate Z values.

Therefore, taking advantage of the quasiclassical approximation made it possible to derive formulas for an exact in η differential cross section of the $\gamma Z \to e^+e^-\gamma' Z$ process, which are not much more complicated than the Born result. It turned out that the Coulomb corrections significantly modify the process cross section and hence must be accounted for in the analysis of available experimental data.

7. Quasiclassical approximation and small-angle scattering at high energies

As was mentioned in a preceding paragraph, the main contribution to the cross sections of various quantum electrodynamics processes in the atomic field at high energies is determined by the small angles between the momenta of initial and final particles, i.e., by large orbital momenta. The application of quasiclassical approach allows us to systematically take account of the contributions from large orbital momenta, as shown in Sections 2–6. Results obtained in the framework of this approach are exact in the parameter $\eta = Z\alpha$. Moreover, consideration of the approximation next-in-order to the leading quasiclassical approximation substantially increases the precision of the results over those obtained in the leading quasiclassical approximation. In this regard, a fundamental difference should be emphasized between the quasiclassical approximation and the eikonal approximation frequently used in describing high-energy processes (see, for instance, book [27]). This difference has been noted already in a study [9], demonstrating that Coulomb corrections to the cross section of e^+e^--pair photoproduction can be obtained in the framework of the quasiclassical but not eikonal approximation. The question arises to what extent it is possible to increase the accuracy of cross section calculations in the framework of the quasiclassical approach. This issue was studied in a recent paper [54] by the example of calculating the small-angle scattering cross section for polarized high-energy particles in the atomic field. The cross section of this process can be represented in the form [27]

$$\frac{d\sigma}{d\Omega} = \frac{1}{2}\frac{d\sigma_0}{d\Omega}\left[1 + S\boldsymbol{\xi}(\boldsymbol{\zeta}_1 + \boldsymbol{\zeta}_2) + T^{ij}\zeta_1^i\zeta_2^j\right], \quad \boldsymbol{\xi} = \frac{\mathbf{p}\times\mathbf{q}}{|\mathbf{p}\times\mathbf{q}|}, \quad (85)$$

where $d\sigma_0/d\Omega$ is the differential cross section for nonpolarized particles, $\mathbf{p}$ and $\mathbf{q}$ are the initial and final electron momenta, $\boldsymbol{\zeta}_1$ is the polarization vector of the initial electron, $\boldsymbol{\zeta}_2$ is the registered polarization vector of the final electron, S is the so-called Sherman function, and T_{ij} is a certain tensor. Cross section $d\sigma_0/d\Omega$ in the leading and the next-to-leading-order scattering angle approximation, $\theta \ll 1$, was known long ago for an arbitrary localized potential $V(r)$ [55]. The cross section can be calculated with such accuracy in the framework of the quasiclassical approach. The Sherman function S calculated in the leading quasiclassical approximation is proportional to θ^2. If S is calculated with the help of a series expansion in η parameter, the contribution leading in η (linear in η) is due to the interference between the scattering amplitudes calculated in the first and second Born approximations [56–60]. Unlike the leading quasiclassical contribution proportional to θ^2, the contribution leading in η is proportional to θ^3 at small θ. There is no conflict between these results, because the expansion of the quasiclassical contribution with respect to η starts with η^2. Thus, the dominant contribution to the Sherman function is given, depending on the η/θ ratio, either by the leading quasiclassical contribution or by the interference between the first and second Born amplitudes. It could be supposed that the $O(\theta^3)$ contribution in the S function corresponds to the next-to-leading-order (quasiclassical correction), i.e., to the contribution from large orbital momenta. However, the case of the Coulomb field considered in Ref. [54] showed that it is absolutely necessary to take account of angular momenta $l \sim 1$ for these terms. It was therefore concluded that it is not possible to go beyond the accuracy of the next-to-leading-order quasiclassical approximation without taking into account the nonquasiclassical contributions corresponding to $l \sim 1$ angular momenta.

7.1 Scattering of polarized electrons in the quasiclassical approximation

For the problem of scattering in the arbitrary localized potential $V(r)$, the asymptotics of the wave function $\psi_{\mathbf{p}}(\mathbf{r})$ at large distances r has the form

$$\psi_{\mathbf{p}}(\mathbf{r}) \approx \exp(i\mathbf{pr})u_{\mathbf{p}} + \frac{\exp(ipr)}{r}(G_0 - \boldsymbol{\alpha}\mathbf{G}_1 - \boldsymbol{\Sigma}\mathbf{G}_2)u_{\mathbf{p}}. \quad (86)$$

Coefficients G_0, $\mathbf{G}_1$, and $\mathbf{G}_2$ are easy to find from the expressions of functions f_0, $\mathbf{f}_1$, and $\mathbf{f}_2$ [see formula (4)]:

$$G_0 = a_0 + \delta a_0, \quad \mathbf{G}_1 = -\frac{\boldsymbol{\Delta}_\perp}{2\varepsilon}(a_0 + \delta a_0 + \delta a_1),$$
$$\mathbf{G}_2 = i\,\frac{\mathbf{q}\times\mathbf{p}}{2\varepsilon^2}\,\delta a_1, \quad (87)$$

where

$$a_0 = -\frac{i\varepsilon}{2\pi}\int d\boldsymbol{\rho}\,\exp(-i\boldsymbol{\Delta}_\perp\boldsymbol{\rho})\left[\exp(-i\chi(\boldsymbol{\rho}) - 1\right],$$
$$\delta a_0 = -\frac{1}{4\pi}\int d\boldsymbol{\rho}\,\exp\left(-i\boldsymbol{\Delta}_\perp\boldsymbol{\rho} - i\chi(\boldsymbol{\rho})\right)\rho\,\frac{\partial}{\partial\rho}\int_{-\infty}^{\infty}dx\,V^2(r_x),$$
$$\delta a_1 = \frac{i}{4\pi\Delta_\perp^2}\int d\boldsymbol{\rho}\,\exp\left(-i\boldsymbol{\Delta}_\perp\boldsymbol{\rho} - i\chi(\boldsymbol{\rho})\right)\boldsymbol{\Delta}_\perp\frac{\boldsymbol{\rho}}{\rho}\frac{\partial}{\partial\rho}\int_{-\infty}^{\infty}dx\,V^2(r_x),$$
$$\chi(\boldsymbol{\rho}) = \int_{-\infty}^{\infty}dx\,V(r_x), \quad r_x = \sqrt{x^2+\rho^2}. \quad (88)$$

Here, $\boldsymbol{\Delta} = \mathbf{q} - \mathbf{p}$, $\mathbf{q} = p\mathbf{r}/r$, and $\boldsymbol{\rho}$ is the two-dimensional vector normal to vector $\mathbf{n}_p = \mathbf{p}/p$ along which the z-axis is directed. For small scattering angles $\theta \ll 1$, one has $\delta a_0 \sim \delta a_1 \sim \theta a_0$. As a result, we arrive at the following expressions for $d\sigma_0/d\Omega$, T^{ij} and S in Eqn (85):

$$\frac{d\sigma_0}{d\Omega} = |a_0|^2\left(1 + 2\,\mathrm{Re}\,\frac{\delta a_0}{a_0}\right), \quad (89)$$
$$T^{ij} = \delta^{ij} + \theta\varepsilon^{ijk}\xi^k,$$
$$S = -\frac{m\theta}{\varepsilon}\,\mathrm{Im}\,\frac{\delta a_1}{a_0}. \quad (90)$$

Equation (89) takes into consideration only the leading and the next-to-leading-order in θ terms in $d\sigma_0/d\Omega$ and T^{ij}, while Eqn (90) takes account of the leading contribution to the Sherman function S. The form of T^{ij} is a simple consequence of helicity conservation in scattering of ultrarelativistic particles.

The condition $|\Delta_z| \approx p\theta^2/2 \ll \Delta_\perp \approx p\theta$ is always fulfilled at small scattering angles. By virtue of this condition, $a_0(\Delta)$ in

Eqn (88) is expressed through coefficient $A_0(\Delta)$ (49):

$$a_0(\Delta) = -\frac{\varepsilon}{2\pi} A_0(\Delta)\,. \tag{91}$$

Due to this relation, the bremsstrahlung cross section in transverse momentum transfers greater than a minimal transfer can be represented in the leading quasiclassical approximation in the form of the product of the scattering cross section and the emission probability [12]. This factorization is violated at small momentum transfers, as well as in the next-to-leading-order quasiclassical approximation (see Section 4).

The expansion for $d\sigma_0/d\Omega$ coincides with that obtained in the eikonal approximation [55]. However, one important remark is in order here [18]. The following formula is usually used in the derivation of the expression for a_0 in the framework of the eikonal approximation:

$$a_0 = -\frac{\varepsilon}{2\pi}\int d\mathbf{r}\, \exp(-i\mathbf{qr})\,V(r)\,\psi^+_{\mathbf{p}}(\mathbf{r}) \tag{92}$$

with $\psi^+_{\mathbf{p}}(\mathbf{r})$ being the eikonal function

$$\psi^{\text{eik}}_{\mathbf{p}}(\mathbf{r}) = \exp\left[i\mathbf{pr} - i\int_0^\infty dx\, V(\mathbf{r} - x\mathbf{n}_p)\right] \tag{93}$$

deduced from the quasiclassical wave function by ignoring quantum fluctuations (see Section 2). Then, the integral over z, ignoring Δ_z by virtue of its smallness compared with $\Delta_\perp$, yields a_0 in Eqn (88). This derivation in the case of the Coulomb field raises questions, since Δ_z is multiplied by $z \sim \rho/\theta$, i.e., $z\Delta_z \sim \rho\Delta_\perp$. If Δ_z is not ignored but the wave function is retained in the eikonal approximation, integration in formula (92) results in the expression for $|a_0|^2$ differing from the correct expression by the presence of an additional factor $2\pi\eta/[\exp(2\pi\eta) - 1]$. If the wave function is taken in the quasiclassical approximation but Δ_z is ignored, integration in formula (92) leads to the expression for $|a_0|^2$ differing from the correct one by an additional factor $2\pi\eta/[1 - \exp(-2\pi\eta)]$. Only retention of Δ_z together with the use of the quasiclassical wave function allows the correct result for a_0 in formula (88) to be obtained from Eqn (92) (see Ref. [18]).

It should be noted that $a_0 \to -a_0^*$, $\delta a_0 \to \delta a_0^*$, and $\delta a_1 \to \delta a_1^*$ in the case of the $V \to -V$ substitution. Due to this, the quasiclassical result for the Sherman function S [Eqn (90)] is invariant with respect to the $V \to -V$ substitution. In contrast, the $2\,\mathrm{Re}\,(\delta a_0/a_0)$ contribution to $d\sigma_0/d\Omega$ in (89) leads to charge asymmetry in scattering, i.e., to the difference between electron and positron scattering cross sections (see, for instance, [27]). For the Coulomb field $V(r) = -\eta/r$, it follows from Eqn (88) that

$$\begin{gathered} a_0 = \frac{2\eta}{\varepsilon\theta^{2-2i\eta}}\,\frac{\Gamma(1-i\eta)}{\Gamma(1+i\eta)}\,, \\ \frac{\delta a_0}{a_0} = \frac{1}{4}\,\pi\theta g^*(\eta)\,, \quad \frac{\delta a_1}{a_0} = -\frac{\pi\theta g^*(\eta)}{4(1+2i\eta)}\,, \end{gathered} \tag{94}$$

where function $g(\eta)$ was defined in Eqn (15). The quasiclassical cross section and function S for the Coulomb field have the form

$$\frac{d\sigma_0}{d\Omega} = \frac{4\eta^2}{\varepsilon^2\theta^4}\left(1 + \frac{\pi\theta}{2}\,\mathrm{Re}\,g(\eta)\right), \tag{95}$$

$$S = -\frac{\pi m\theta^2}{4\varepsilon}\,\mathrm{Im}\,\frac{g(\eta)}{1-2i\eta}\,. \tag{96}$$

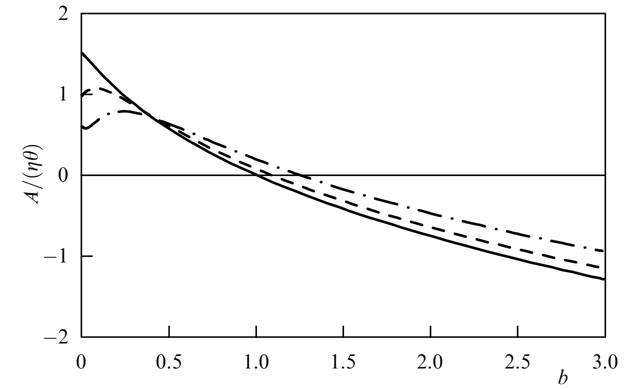

Figure 25. Asymmetry A (99) in units of $\eta\theta$ as a function of $b = \theta\varepsilon R$ for $\eta = 0.1$ (solid curve), $\eta = 0.4$ (dashed curve), and $\eta = 0.7$ (dash-dotted curve).

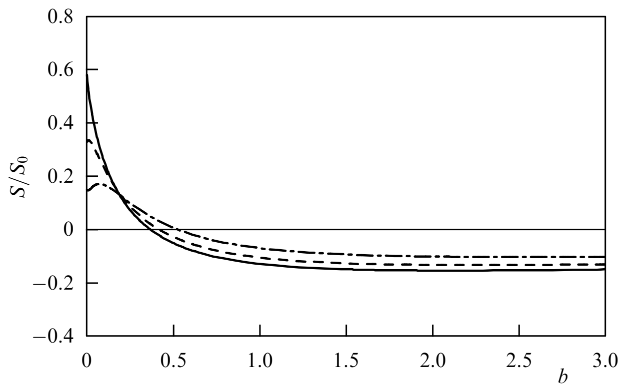

Figure 26. Sherman function S (100) in $S_0 = m\eta^2\theta^2/\varepsilon$ units depending on $b = \theta\varepsilon R$ for $\eta = 0.1$ (solid curve), $\eta = 0.4$ (dashed curve), and $\eta = 0.7$ (dash-dotted curve).

In other words, the quasiclassical Sherman function is proportional to θ^2, while Mott's famous result [56] for the leading contributions to S in η is proportional to $\theta^3\ln\theta$. For this reason, Mott's result is inapplicable for $\theta \lesssim \eta$.

Let us discuss now the finite nucleus size effect on the $d\sigma_0/d\Omega$ cross section and the Sherman function S making use of the model potential

$$V(r) = -\frac{\eta}{\sqrt{r^2 + R^2}}\,, \tag{97}$$

where R is the characteristic nucleus size. Since all integrals in Eqn (88) are taken for this potential, one obtains

$$\frac{d\sigma_0}{d\Omega} = \frac{4\eta^2}{\varepsilon^2\theta^4}\left|\frac{bK_{1-i\eta}(b)}{\Gamma(1+i\eta)}\right|^2 (1+A)\,, \tag{98}$$

$$A = \frac{\pi\eta\theta}{2}\,\mathrm{Re}\,\frac{\Gamma(1+i\eta)\big(2K_{1/2-i\eta}(b) - bK_{3/2-i\eta}(b)\big)}{\Gamma(3/2+i\eta)\sqrt{2b}\,K_{1-i\eta}(b)}\,, \tag{99}$$

$$S = \frac{\pi\eta m\theta^2}{4\varepsilon}\,\mathrm{Im}\,\frac{\Gamma(1+i\eta)K_{1/2-i\eta}(b)}{\Gamma(3/2+i\eta)\sqrt{2b}\,K_{1-i\eta}(b)}\,, \quad b = \theta\varepsilon R\,, \tag{100}$$

where $K_\nu(x)$ is the modified Bessel function of the second kind. Quantity A in Eqn (99) stands for charge asymmetry

$$A = \frac{d\sigma_0(\eta) - d\sigma_0(-\eta)}{d\sigma_0(\eta) + d\sigma_0(-\eta)}\,. \tag{101}$$

In the $b \to 0$ limit, the deduced formulas (98) and (100) coincide with (95) and (96). Figures 25 and 26 plot asymmetry A and function S depending on b for several η values. Both functions show a strong dependence on b and η. Interestingly, they change the sign at $b \sim 1$. This property can be expected to manifest itself for usual parametrizations of the nuclear electrical potential.

7.2 Small-angle expansion of the exact Coulomb scattering amplitude

The amplitude of electron scattering in the Coulomb field is known exactly in η for any electron energies and scattering angles (see, for example, monographs [4, 27]):

$$M_{\mathrm{fi}} = \frac{\mathrm{i}}{2p}\,\phi_{\mathrm{f}}^{\dagger}\left[G(\theta) - \frac{\mathrm{i}\eta m}{p}\,F(\theta) - \mathrm{i}\left(G(\theta)\tan\frac{\theta}{2} + \frac{\mathrm{i}\eta m}{p}\,F(\theta)\cot\frac{\theta}{2}\right)\boldsymbol{\xi}\boldsymbol{\sigma}\right]\phi_{\mathrm{i}}\,,$$

where ϕ_{i} and ϕ_{f} are the spinors corresponding to the initial and final electrons, respectively, and functions $F(\theta)$ and $G(\theta)$ have the form

$$F(\theta) = -\sum_{l=1}^{\infty}\frac{\Gamma(\gamma_l - \mathrm{i}\nu)}{\Gamma(\gamma_l + \mathrm{i}\nu + 1)}\exp\left[\mathrm{i}\pi(l-\gamma_l)\right] l\,(P_l - P_{l-1})\,, \tag{102}$$

$$G(\theta) = -\cot\frac{\theta}{2}\,\frac{\mathrm{d}F}{\mathrm{d}\theta}\,. \tag{103}$$

Here, $P_l = P_l(\cos\theta)$ are the Legendre polynomials, and $\gamma_l = \sqrt{l^2-\eta^2}$. If the amplitude is known exactly, it is possible to study the nontrivial interplay between contributions from large orbital momenta l (the quasiclassical contribution) and contribution from $l \sim 1$ to the cross section and the Sherman function for electron scattering in the Coulomb field. For small scattering angles θ, the main contribution to the scattering amplitude is determined by angular momenta $l \gg 1$ not only in the ultrarelativistic case, but also at arbitrary $\beta = p/\varepsilon$. Therefore, parameters $\eta = Z\alpha$ and $\nu = Z\alpha/\beta$ are regarded as independent in this section. We shall consider the small-angle expansion regardless of fulfillment of the condition $\eta \ll 1$ assumed in Ref. [60].

The differential cross section for nonpolarized particles $\mathrm{d}\sigma_0/\mathrm{d}\Omega$ and the Sherman function $S(\theta)$ expressed through $F(\theta)$ and $G(\theta)$ take the form

$$\frac{\mathrm{d}\sigma_0}{\mathrm{d}\Omega} = \frac{1}{4p^2}\left[\frac{|G(\theta)|^2}{\cos^2(\theta/2)} + \frac{\eta^2 m^2 |F(\theta)|^2}{p^2\sin^2(\theta/2)}\right], \tag{104}$$

$$S(\theta) = \frac{\eta m p\sin\theta\,\mathrm{Re}\,FG^*}{|G(\theta)|^2 p^2\sin^2(\theta/2) + \eta^2 m^2 |F(\theta)|^2\cos^2(\theta/2)}\,.$$

Reference [54] reports on the following representation for function $F(\theta)$ as $\theta \ll 1$:

$$F \approx F_{\mathrm{QC}} + \delta F\,, \tag{105}$$

$$F_{\mathrm{QC}} = \frac{\Gamma(1-\mathrm{i}\nu)}{\Gamma(1+\mathrm{i}\nu)}\,s^{2\mathrm{i}\nu}\left[1 + \frac{\mathrm{i}\pi\eta^2}{(1+2\mathrm{i}\nu)\nu}\,g^*(\nu)s + \frac{\mathrm{i}\eta^2}{2(1+\mathrm{i}\nu)\nu}\left(1 + 2\mathrm{i}\nu - \frac{\pi^2\eta^2}{4}\right)s^2\right],$$

$$\delta F = \frac{\Gamma(1-\mathrm{i}\nu)}{\Gamma(1+\mathrm{i}\nu)}\,C(\eta,\nu)s^2\,.$$

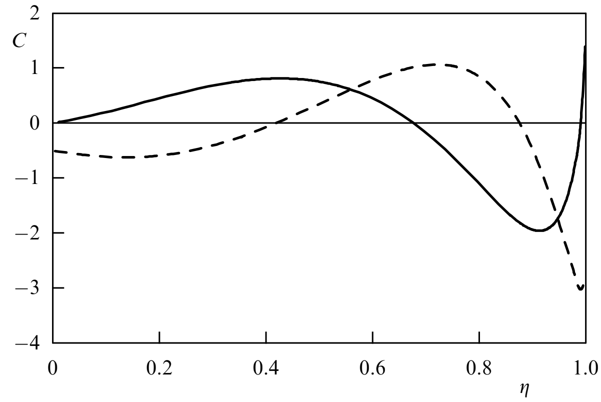

Figure 27. Real (solid curve) and imaginary (dashed curve) parts of function $C(\eta,\nu)$ [Eqn (106)] at $\nu = \eta$ as a function of η.

Here, the notations were used:

$$C(\eta,\nu) = -\mathrm{i}\eta^2\left[\frac{1}{2\nu} + \mathrm{i} + \frac{\pi}{2(1-2\mathrm{i}\nu)} - \frac{\pi^2\eta^2}{8\nu}\right] + \frac{\Gamma(1+\mathrm{i}\nu)}{\Gamma(1-\mathrm{i}\nu)}\sum_{l=1}^{\infty}2l^2\left[\frac{\Gamma(\gamma_l-\mathrm{i}\nu)\exp\left[\mathrm{i}\pi(l-\gamma_l)\right]}{\Gamma(\gamma_l+\mathrm{i}\nu+1)} - \frac{\Gamma(l-\mathrm{i}\nu)}{\Gamma(l+\mathrm{i}\nu+1)}\,T_l\right],$$
$$T_l = 1 + \frac{\mathrm{i}\pi}{2l}\,\eta^2 + \frac{\eta^2}{2l^2}\left(1 + 2\mathrm{i}\nu - \frac{\pi^2\eta^2}{4}\right), \tag{106}$$

where $s = \sin(\theta/2)$. The term F_{QC} is determined by the contribution from large l (the quasiclassical contribution), and the sum over l in the term δF converges at $l \sim 1$ (the nonquasiclassical contribution). Function $C(\eta,\nu)$ shows strong dependence on η and ν. This inference is confirmed in Fig. 27, in which both real and imaginary parts of the function $C(\eta,\nu)$ at $\nu = \eta$ ($\beta = 1$) are depicted as a function of η.

Substituting formula (105) into (104) gives

$$\frac{\mathrm{d}\sigma_0}{\mathrm{d}\Omega} = \frac{\nu^2}{4p^2 s^4}\left[1 + \pi\beta^2\,\mathrm{Re}\,g(\nu)s - 2\nu^{-1}\,\mathrm{Im}\left(s^{2\mathrm{i}\nu}C^*(\eta,\nu)\right)s^2\right], \tag{107}$$

$$S(\theta) = \frac{ms^2}{\varepsilon\nu}\left\{-\pi\eta\beta\,\mathrm{Im}\left(\frac{g(\nu)}{1-2\mathrm{i}\nu}\right) + \left[\frac{\eta^2}{1+\nu^2}\left(1 - \frac{3\pi^2\eta^2}{4(1+4\nu^2)}\right) + \pi^2\eta\beta^3\,\mathrm{Im}\left(\frac{g(\nu)}{1-2\mathrm{i}\nu}\right)\mathrm{Re}\,g(\nu) - 2\,\mathrm{Re}\left[(1+\mathrm{i}\nu)s^{2\mathrm{i}\nu}C^*(\eta,\nu)\right]\right]s\right\}. \tag{108}$$

The second correction to the cross section originates from interference between quasiclassical and nonquasiclassical contributions to the amplitude. This means that this correction cannot be obtained in the framework of the quasiclassical approach. It was shown in Ref. [18] that the amplitude of elastic small-angle scattering of electrons at high energies obtained in the framework of the quasiclassical approach taking account of the first-order quasiclassical correction coincides with the amplitude obtained in the eikonal approach taking into consideration the first-order correction. The eikonal approach allows us to perform regular expansion of the wave function [61, 62]. Hence, the question may be raised: is it possible to obtain the $O(s^2)$ contribution to Eqn (107) in the framework of the eikonal approach? The answer: certainly not. Indeed, the eikonal scattering amplitude for $\Delta_\perp \neq 0$ takes the form

$$M_{\mathrm{fi}} = -\frac{\mathrm{i}p}{2\pi}\int \mathrm{d}\boldsymbol{\rho}\,\exp\left(-\mathrm{i}\boldsymbol{\Delta}_\perp\boldsymbol{\rho} - \mathrm{i}\chi_0(\boldsymbol{\rho})\right) \times \phi_{\mathrm{f}}^\dagger\left[1 - \mathrm{i}\chi_1 - \mathrm{i}\chi_2 - \frac{\chi_1^2}{2} + \ldots\right]\phi_{\mathrm{i}}\,. \qquad (109)$$

In the Coulomb field, $\chi_0 = 2\nu\ln p\rho$. It follows from dimensional considerations that eikonal corrections have the form $\chi_{n>0}(\rho) = \mathcal{P}_n(\ln p\rho)/(p\rho)^n$, where $\mathcal{P}_n(x)$ are certain polynomials with matrix coefficients. Substituting variables $\boldsymbol{\rho} \to (2/\Delta_\perp)\boldsymbol{\rho}$ leads to

$$M_{\mathrm{fi}} = -s^{2\mathrm{i}\nu}\,\frac{2\mathrm{i}p}{\pi\Delta_\perp^2}\int \mathrm{d}\boldsymbol{\rho}\,\exp\left(-2\mathrm{i}\boldsymbol{\delta\rho}\right)\rho^{-2\mathrm{i}\nu}\phi_{\mathrm{f}}^\dagger\left\{1 - \mathrm{i}\,\frac{s}{\rho}\,\mathcal{P}_1\left(\ln\frac{\rho}{s}\right) - \frac{s^2}{\rho^2}\left[\mathrm{i}\mathcal{P}_2\left(\ln\frac{\rho}{s}\right) + \frac{1}{2}\,\mathcal{P}_1^2\left(\ln\frac{\rho}{s}\right)\right] + \ldots\right\}\phi_{\mathrm{i}}\,, \qquad (110)$$

where $\boldsymbol{\delta} = \boldsymbol{\Delta}_\perp/\Delta_\perp$ is the unit vector. Taking the integral over $\boldsymbol{\rho}$ yields amplitude M_{fi} in the eikonal approximation:

$$M_{\mathrm{fi}} = \frac{\Gamma(1-\mathrm{i}\nu)}{\Gamma(1+\mathrm{i}\nu)}\,s^{2\mathrm{i}\nu}\,\frac{\nu}{2ps^2} \times \phi_{\mathrm{f}}^\dagger\left[1 + s\mathcal{Q}_1(\ln s) + s^2\mathcal{Q}_2(\ln s) + \ldots\right]\phi_{\mathrm{i}}\,, \qquad (111)$$

where $\mathcal{Q}_1$ and $\mathcal{Q}_2$ are certain polynomials with coefficients that are functions of ν and η. The common phase factor $s^{2\mathrm{i}\nu}$ disappears in $|M_{\mathrm{fi}}|^2$, which means that Eqn (111) cannot reproduce the oscillating factor $\mathrm{Im}\,[s^{2\mathrm{i}\nu}C^*(\eta,\nu)]$ in Eqn (107). This is not surprising, bearing in mind that the condition for the applicability of the eikonal approximation is violated at small distances.

Let us discuss the nontrivial relation between amplitudes obtained by small-angle expansion and by a series expansion in small ν. Retaining only the leading terms in ν in the expansion of coefficients with respect to s yields

$$\frac{\mathrm{d}\sigma_0}{\mathrm{d}\Omega} = \frac{\nu^2}{4p^2s^4}\left(1 + s\pi\eta\beta - s^2\beta^2\right), \qquad (112)$$

$$S(\theta) = \frac{2\eta m s^2}{\varepsilon}\left[\pi\eta(2\ln 2 - 1) + \beta s\ln s\right]. \qquad (113)$$

Cross section (112) is consistent with the small-angle expansion of results obtained in Refs [57, 58], and function S [Eqn (113)] with the small angle-expansion of the expression for the Sherman function from Ref. [59]. The term proportional to $s\ln s$ in formula (113) is in agreement with the known Mott result [56].

Evidently, the relative values of the first-order and second-order corrections in s to the differential cross section are proportional to the ratio of two small parameters, ν/θ, that can be either larger or smaller than unity. An analogous situation takes place for the Sherman function, i.e., the ratio between the leading quasiclassical contribution and the correction is proportional to $\nu/(\theta\ln\theta)$.

Result (105) was obtained in the small-angle scattering approximation, $\theta \ll 1$. However, it turned out that expression (105) for function F is surprisingly well consistent with the exact function (102) for all θ. Therefore, the use of Eqns (103) and (105) in (104) allows obtaining very good approximations for the cross section and the Sherman function over the entire range of angles and nuclear charges. This inference is illustrated in Fig. 28 showing the scattering cross section for an ultrarelativistic particle on the lead nucleus ($Z = 82$) as a function of $s = \sin(\theta/2)$. This correspondence disappears at large scattering angles if contributions on the order of s^2 (dotted curve) in Eqn (105) are ignored.

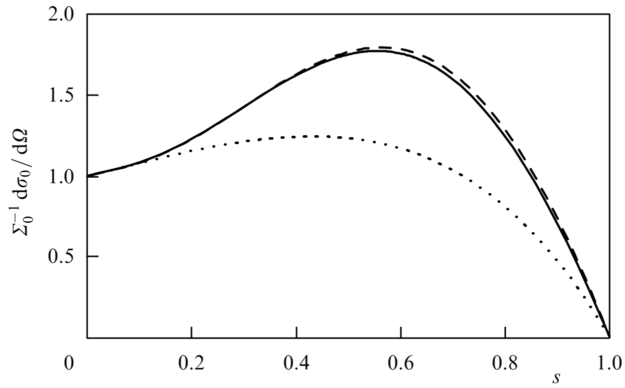

Figure 28. Dependence of differential cross section $\mathrm{d}\sigma_0/\mathrm{d}\Omega$ [Eqn (104)] in units of $\Sigma_0 = \nu^2/(4p^2s^4)$ on $s = \sin(\theta/2)$ for $\varepsilon \gg m$ and $\nu = \eta = 0.6$. Solid curve — exact result obtained from Eqns (102) and (103), dashed curve — result obtained from Eqns (103) and (105), dotted curve — result obtained from F in the quasiclassical approximation taking account of the first-order quasiclassical correction (defined by formula (105) with terms $\propto s^2$ dropped).

8. Conclusion

This review summarizes current research on fundamental quantum electrodynamics processes whereby high-energy particles interact with atoms. It is of importance for various applications that the cross sections of these processes be known exactly. It is shown that the employment of the quasiclassical approach permits in all cases obtaining results exact in parameter $\eta = Z\alpha$, the form of which is not much more complicated than that of the respective results obtained in the Born approximation. Calculations in the next-to-leading-order quasiclassical approximation permit us not only to deduce formulas fairly exact at intermediate energies but also to quantitatively predict for the first time such phenomena as charge asymmetry in the photoproduction and bremsstrahlung processes proceeding in an atomic field at high energies of impact particles.

The study was supported by the Russian Science Foundation (grant 14-50-00080).

References

1. Dirac P A M *Proc. R. Soc. London A* **117** 610 (1928)
2. Bethe H, Heitler W *Proc. R. Soc. London A* **146** 83 (1934)
3. Racah G *Nuovo Cimento* **11** 461 (1934)
4. Berestetskii V B, Lifshitz E M, Pitaevskii L P *Quantum Electrodynamics* (Oxford: Pergamon Press, 1982); Translated from Russian: *Kvantovaya Elektrodinamika* (Moscow: Nauka, 1989)
5. Øverbø I, Mork K J, Olsen H A *Phys. Rev.* **175** 1978 (1968)
6. Sud K K, Sharma D K *Rad. Phys. Chem.* **75** 631 (2006)
7. Bethe H A, Maximon L C *Phys. Rev.* **93** 768 (1954)
8. Davies H, Bethe H A, Maximon L C *Phys. Rev.* **93** 788 (1954)
9. Olsen H A, Maximon L C, Wergeland H *Phys. Rev.* **106** 27 (1957)
10. Furry W *Phys. Rev.* **46** 391 (1934)
11. Sommerfeld A, Maue A W *Ann. Phys.* **22** 629 (1935)

12. Baier V N, Katkov V M, Fadin V S *Izluchenie Relyativistskikh Elektronov* (Emission of Relativistic Electrons) (Moscow: Atomizdat, 1973)
13. Baier V N, Katkov V M, Strakhovenko V M *Electromagnetic Processes at High Energies in Oriented Single Crystals* (Singapore: World Scientific, 1998); Translated from Russian: *Elektromagnitnye Protsessy pri Vysokoi Energii v Orientirovannykh Monokristallakh* (Novosibirsk: Nauka, 1989)
14. Mil'shtein A I, Strakhovenko V M *Phys. Lett. A* **95** 135 (1983)
15. Mil'shtein A I, Strakhovenko V M *Sov. Phys. JETP* **58** 8 (1983); *Zh. Eksp. Teor. Fiz.* **85** 14 (1983)
16. Lee R N, Milstein A I *Phys. Lett. A* **198** 217 (1995)
17. Lee R N, Milstein A I *JETP* **80** 777 (1995); *Zh. Eksp. Teor. Fiz.* **107** 1393 (1995)
18. Lee R N, Milstein A I, Strakhovenko V M *JETP* **90** 66 (2000); *Zh. Eksp. Teor. Fiz.* **117** 75 (2000)
19. Di Piazza A, Milstein A I *Phys. Lett. B* **717** 224 (2012)
20. Krachkov P A, Milstein A I *Phys. Rev. A* **91** 032106 (2015)
21. Milstein A I, Schumacher M *Phys. Rep.* **243** 183 (1994)
22. Akhmadaliev Sh Zh et al. *Phys. Rev. C* **58** 2844 (1998)
23. Lee R N et al. *Phys. Rep.* **373** 213 (2003)
24. Akhmadaliev Sh Zh et al. *Phys. Rev. Lett.* **89** 061802 (2002)
25. Downie E J et al. *Phys. Lett. B* **728** 645 (2014)
26. Lee R N, Milstein A I, Strakhovenko V M *Phys. Rev. A* **85** 042104 (2012)
27. Überall H *Electron Scattering From Complex Nuclei* (Pure and Applied Physics, Vol. 36A) (New York: Academic Press, 2012)
28. Hubbell J H, Gimm H A, Øverbø I *J. Phys. Chem. Rev. Data* **9** 1023 (1980)
29. Hubbell J H *Rad. Phys. Chem.* **59** 113 (2000)
30. Øverbø I *Phys. Lett. B* **71** 412 (1977)
31. Lee R N, Milstein A I, Strakhovenko V M *Phys. Rev. A* **69** 022708 (2004)
32. Di Piazza A, Milstein A I *Phys. Rev. A* **82** 042106 (2010)
33. Ivanov D, Melnikov K *Phys. Rev. D* **57** 4025 (1998)
34. Hencken K, Kuraev E A, Serbo V G *Phys. Rev. C* **75** 034903 (2007)
35. Jentschura U D, Serbo V G *Eur. Phys. J. C* **64** 309 (2009)
36. Brodsky S J, Gillespie J R *Phys. Rev.* **173** 1011 (1968)
37. Mil'shtein A I, Strakhovenko V M *JETP* **76** 775 (1993); *Zh. Eksp. Teor. Fiz.* **103** 1584 (1993)
38. Rohrlich F *Phys. Rev.* **108** 169 (1957)
39. Sherman N K, Ross C K, Lokan K H *Phys. Rev. C* **21** 2328 (1980)
40. Rosenblum E S, Shrader E F, Warner R M (Jr.) *Phys. Rev.* **88** 612 (1952)
41. Gimm H A, Hubbell J H, National Bureau of Standards (U.S.) Technical Note No. 968 (Washington, D.C.: U.S. GPO, 1978)
42. Di Piazza A, Milstein A I *Phys. Rev. A* **85** 042107 (2012)
43. Deck R T, Moroi D S, Alling W R *Nucl. Phys. A* **133** 321 (1969)
44. Olsen H *Phys. Rev.* **99** 1335 (1955)
45. Olsen H, Maximon L C *Phys. Rev.* **114** 887 (1959)
46. Lee R N, Milstein A I, Strakhovenko V M, Schwarz O Ya *JETP* **100** 1 (2005); *Zh. Eksp. Teor. Fiz.* **127** 5 (2005)
47. Korol A V *J. Phys. B* **26** 3137 (1993)
48. Krylovetskii A A et al. *JETP* **95** 1006 (2002); *Zh. Eksp. Teor. Fiz.* **122** 1168 (2002)
49. Smirnov A I *Sov. J. Nucl. Phys.* **25** 548 (1977); *Yad. Fiz.* **25** 1030 (1977)
50. Krachkov P A, Lee R N, Milstein A I *Phys. Rev. A* **91** 062109 (2015)
51. Huld B *Phys. Lett. B* **24** 185 (1967)
52. Corbò G *Phys. Rev. D* **17** 725 (1978)
53. Krachkov P A, Lee R N, Milstein A I *Phys. Rev. A* **90** 062112 (2014)
54. Krachkov P A, Lee R N, Milstein A I *Phys. Lett. B* **751** 284 (2015)
55. Akhiezer A I, Boldyshev V F, Shul'ga N F *Theor. Math. Phys.* **23** 311 (1975); *Teor. Mat. Fiz.* **23** 11 (1975)
56. Mott N F *Proc. R. Soc. London A* **124** 425 (1929)
57. McKinley W A (Jr.), Feshbach H *Phys. Rev.* **74** 1759 (1948)
58. Dalitz R H *Proc. R. Soc. London A* **206** 509 (1951)
59. Johnson W R, Weber T A, Mullin C J *Phys. Rev.* **121** 933 (1961)
60. Gluckstern R L, Lin S-R *J. Math. Phys.* **5** 1594 (1964)
61. Wallace S J *Phys. Rev. D* **8** 1846 (1973)
62. Tjon J A, Wallace S J *Phys. Rev. C* **74** 064602 (2006)